Expedition 313 summary[1]

Expedition 313 Scientists[2]

Chapter contents

Abstract

Integrated Ocean Drilling Program (IODP) Expedition 313 to the New Jersey Shallow Shelf off the east coast of the United States is the third IODP expedition to use a mission-specific platform. It was conducted by the European Consortium for Ocean Research Drilling (ECORD) Science Operator (ESO) between 30 April and 17 July 2009, with additional support from the International Continental Scientific Drilling Program (ICDP). There were three objectives: (1) date late Paleogene–Neogene depositional sequences and compare ages of unconformable surfaces that divide these sequences with times of sea level lowerings predicted from the $\delta^{18}O$ glacio-eustatic proxy; (2) estimate the corresponding amplitudes, rates, and mechanisms of sea level change; and (3) evaluate sequence stratigraphic facies models that predict depositional environments, sediment compositions, and stratal geometries in response to sea level change. We drilled at three locations in around 35 m of water 45–67 km offshore, targeting the topsets, foresets, and toesets of several clinoforms at 180–750 meters below seafloor (mbsf). Seismic correlations to previously drilled holes on the continental slope and extrapolations of depths to key horizons in wells drilled into the adjacent coastal plain suggest the clinoform structures investigated during Expedition 313 were deposited during times of oscillations in global sea level; however, this needs to be determined with much greater certainty. The age, lithofacies, and core-log-seismic correlations provided by drilling at key locations will yield the data needed for a rigorous evaluation. We attempted 612 core runs with 80% recovery totaling 1311 m in length. Some or all of the upper 180–280 m of sand-prone sediment was drilled without coring. The deepest hole (M0029A) reached 757 mbsf, and the oldest sediment recovered was late Eocene (Hole M0027A). Wireline logs gathered spectral gamma ray, resistivity, magnetic susceptibility, sonic, and acoustic televiewer data; a vertical seismic profile was run at each site. Multisensor core logger (MSCL), natural gamma ray, and thermal conductivity measurements were made on all cores prior to splitting. Aided by physical properties of discrete samples measured onshore, we have established preliminary core-log-seismic ties with depth uncertainties typically ±7 m or less. We are confident that further study will narrow this range and firmly link facies successions to as many as 16 surfaces and/or sequence-bounding unconformities mapped in the regional seismic grid. Eight lithologic units are recognized that contain important

physical and biofacies indicators of paleobathymetry. Reliable zonations of multiple fossil groups, Sr isotopic ages measured on mollusks and foraminifers, and intervals of magnetic reversal chronology provide a nearly continuous composite record of ~1 m.y. sea level cycles (22–12 Ma). Shifts in climate on the adjacent coastal plain provide distinct pollen markers in all three holes and represent another correlation tool. We recovered regressive sediment bodies that are absent in onshore boreholes because of those updip locations. Lithofacies and benthic foraminifer assemblages provide a rich source of information concerning depositional setting and imply as much as 60 m water depth changes; calculations of sediment compaction, crustal loading, and other corrections need to be made before we can estimate the corresponding magnitudes of eustatic change. Large variations in pore water salinity appear to be controlled by lithofacies. Their sharp vertical gradients await explanation, and relationships to microbiologic communities that we recovered from unsplit cores have yet to be determined.

Introduction

Shallow-water drilling—a new beginning

The formation of the Deep Sea Drilling Project (DSDP) in 1968 began an era of scientific exploration that has revolutionized our understanding of how Earth works. With bold ambitions, a converted drillship, and an innovative planning structure, geologists and geophysicists set out to retrieve hard facts from wherever their scientific questions led them. Four decades later, we are still mining knowledge from the ocean basins with objectives, tools, and management features that have direct ties back to those prescient architects of the DSDP.

Despite successes in deep water, the difficulty in ensuring the ability to drill safely and effectively in shallow water left a large blank spot in our understanding of fundamental Earth processes. This was not a matter of oversight or inadequate technology; DSDP purposely set out to explore the rich frontier of the deep ocean floor in the best manner possible, and that required using a drillship that was inappropriate for shallow-water objectives. Until 2003, earth scientists were confronted with a situation similar to what they had faced prior to 1968: we had uncovered tantalizing questions (concerning decadal climate change, land-sea links across shoreline systems, and factors that control the discontinuous buildup of shallow-water sediments, to name just three), but until that time there was no international means of organizing a way to pursue these questions.

The Integrated Ocean Drilling Program (IODP) was conceived, in part, to address this need for more mission-oriented technology. This strategy has proved very successful, leading to breakthroughs in understanding previously unattainable objectives in complex, deeply buried seismogenic zones (Nankai Trough; IODP Expeditions 314/315/316, 319, and 322); ice-covered regions (the Arctic Ocean; IODP Expedition 302); and environmentally sensitive modern reefs (Tahiti; IODP Expedition 310) (Kinoshita, Tobin, Ashi, Kimura, Lallemant, Screaton, Curewitz, Masago, Moe, et al., 2009; Saffer, McNeill, Araki, Byrne, Eguchi, Toczko, Takahashi, et al., 2009; Underwood, Saito, Kubo, et al., 2009; Backman, Moran, McInroy, Mayer, et al., 2006; Camoin, Iryu, McInroy, et al., 2007). The New Jersey margin, because its geology is known and is easily accessible, is an especially attractive location for documenting sedimentation during times of large sea level change. Equipped with mission-specific platforms, the time is now for the ocean science community to make fundamental discoveries concerning the workings of this complex and a fundamental set of Earth processes.

Eustasy as a global phenomenon

Understanding the history, cause, and impact of sea level change is a compelling goal of Earth system research. There is worldwide evidence of encroaching shorelines today, with the added concern that the rate of this change has been increasing over the last 50 y: ~1.8 mm/y in the last half of the twentieth century (Church and White, 2006) and ~3 mm/y at present (Cazenave et al., 2009). In many coastal regions, the rate of rise is even higher because of the additional effect of local subsidence. Although this may be in part a natural pattern, there is overwhelming scientific evidence indicating this rate increase is due to human activities. The geologic record shows that global sea level has fluctuated by well over 100 m at rates as high as 20–40 mm/y (summaries in Donovan et al., 1979; Fairbanks, 1989; Stanford et al., 2006) at various times in Earth's history. Clearly we must learn about these past events if we are to prepare in any sensible manner for the sea level increase ahead of us.

IODP Expedition 313 does not address the centennial scale of eustatic variation; for that, strategies synthesizing tide gauge histories and Holocene marsh records are required. Instead, this study leads toward a broader understanding of the long-term behavior and wide-ranging effects of changes in the divide between land and sea. Throughout Earth's history, the transfer of energy and material across this

boundary has profoundly influenced the interactions between the lithosphere, biosphere, and atmosphere and continues to affect the balance of these systems today. Weathering rates, sediment distribution, stratal architecture, carbon burial, and glaciation are just a few of the many processes intertwined with eustatic change.

Despite its importance, knowledge of the basic amplitudes and rates of sea level variations on timescales of tens of thousands to millions of years is surprisingly limited. Our goal is to address this deficiency in the way endorsed by several study groups (e.g., Imbrie et al., 1987; JOIDES SL-WG, 1992; Quinn and Mountain, 2000): by sampling key facies across the prograding deposits of a passive continental margin, such as New Jersey.

Distinguishing eustasy from the effects of subsidence and changing sediment supply requires a fundamental understanding of passive margin response to sedimentation. Deposits adjacent to the shoreline are replete with stratal discontinuities on all spatial scales, including sequence boundaries and regional unconformities associated with evidence for base-level lowering (Vail et al., 1977; Posamentier et al., 1988). Sequence boundaries provide a means to objectively subdivide the stratigraphic record (Christie-Blick et al., 1990; Christie-Blick, 1991; Miall, 1991; Catuneanu et al., 2009), and the intervening sedimentary sequences provide the basis for evaluating controls on sedimentary architecture and predicting sedimentary facies and societally important resource distributions (e.g., hydrocarbons and potable water; Vail et al., 1977; Sugarman et al., 2006). Remarkably similar sequence architecture occurs on margins of widely contrasting tectonic and sedimentary histories (e.g., Bartek et al., 1991), emphasizing the fact that eustasy exerts a fundamental, worldwide control on the stratigraphic record. Nevertheless, it is clear that tectonism and changes in sediment supply also have molded the stratigraphic record (e.g., Reynolds et al., 1991); the challenge is to isolate the imprint of each of these influences.

Sequence stratigraphy provides a powerful tool for deciphering margin records, and many recent papers show the interest of the community in developing this approach (Catuneanu et al., 2009; Embry, 2008–2009; Neal and Abreu, 2009). But the fact remains that many of its fundamental assumptions have not been tested. For example, although the facies models of the Exxon Production Research Company (EPR) (e.g., Posamentier et al., 1988) are widely applied, the nature of facies associated with prograding clinoforms has not been documented (although participants of Ocean Drilling Program [ODP] Legs 166 and 174A made contributions to understanding facies associated with clinoforms). Furthermore, the timing and phase relationships of facies distributions with respect to sea level change have not been evaluated (e.g., Reynolds et al., 1991). More importantly, the sequence stratigraphic record has been used to extract a eustatic history, despite the fact that critical assumptions (e.g., the water depth at the lowest point of onlap; Greenlee and Moore, 1988; see discussion below) have not been proven.

Eustatic unknowns: amplitude, response, and mechanism

Measuring the geologic record of amplitudes of eustatic change is a difficult task. Although deep-sea $\delta^{18}O$ records provide precise timing of glacio-eustatic changes (Miller et al., 1991, 1996b, 2005a), eustatic amplitudes can be estimated using $\delta^{18}O$ to no better than ±20% for the past few million years and ±50% prior to that because of assumptions about paleotemperature and application of the Pleistocene sea level/δ_w calibration of Fairbanks and Matthews (1978) to the older record (Miller et al., 2005a). Carbonate atolls have been sampled as fossil "dip sticks" (e.g., ODP Legs 143 and 144), and although this approach has been successful for the Pleistocene (Fairbanks, 1989; Camoin, Iryu, McInroy, et al., 2007), recovery and age control for records older than the late Pleistocene have posed very large challenges. Continental margin sediments have long been regarded as a viable source for extracting eustasy (e.g., Vail et al., 1977; Watts and Steckler, 1979; Haq et al., 1987; Greenlee and Moore, 1988), though the effects of total subsidence (compaction, loading, and cooling) as well as changes in sediment supply must be estimated.

Various facies models have been proposed to explain shelf sedimentation in response to eustatic changes (e.g., Posamentier et al., 1988; Galloway, 1989a, 1989b; and Embry, 2008–2009, among others), but the fact remains that the response of passive margin sedimentation to large, rapid sea level changes is poorly known. One of the main reasons for this lack of information is the scarcity of direct sampling of well-imaged seismic sequences in the regions most affected by sea level change. Understanding the amplitude of sea level change and the sedimentary response requires knowledge of the depositional setting of strata that onlap sequence boundaries. Without samples, it cannot be known if this onlap is coastal, marginal marine, or deep marine (~100 m or more, as suggested by Greenlee and Moore, 1988). Furthermore, the depositional significance (e.g., shoreface versus midshelf) of the clinoform inflection point, a critical element in facies interpretation, has been inferred mostly through forward models,

although tantalizing evidence recovered at ODP Hole 1071F (Leg 174A) suggests a marginal marine setting ~3.5 km landward of one upper middle Miocene clinoform inflection point (Austin, Christie-Blick, Malone, et al., 1998). Although continued analysis of Leg 174A sequences may shed new light on shelf facies models and their predictions from seismic data, these drilling results were limited by low core recovery and penetration of only upper middle Miocene and younger strata, hampering efforts to establish reliable facies models. Drilling in Holes M0027A–M0029A provides information needed to properly evaluate these depositional facies models.

The importance of eustasy versus tectonism to the formation and preservation of sequences is a long-standing debate addressed by Expedition 313. Tectonism in this context includes phenomena that operate across a large range of scales in both time and space (i.e., from rapid, narrowly focused "active" processes such as faulting and salt intrusion to the slower and more laterally extensive "passive" process of flexural loading). Backstripping analyses at 11 onshore boreholes (Kominz et al., 1998, 2008; Van Sickel et al., 2004; see summary in Miller et al., 2005b) have shown that active tectonism has played a minimal role in Cenozoic onshore deposition. By contrast, backstripping has shown ~30 m of excess subsidence at onshore Delaware wells versus corresponding wells in New Jersey because of the flexural load of 21–12 m.y. old sediments offshore Delaware (Browning et al., 2006). From this and other evidence these workers concluded the following:

1. Eustatic change is a first-order control on accommodation space and provides a simultaneous imprint on all continental margins.
2. Although tectonic movement of the crust can result in large stratigraphic gaps, no evidence of this effect is detected in Miocene sequences from New Jersey.
3. Second-order differences in sequences can be attributed to local flexural loading, particularly in regions that experienced large-scale progradation.

Background

Several features of the New Jersey margin make it an ideal location to investigate the late Cenozoic history of sea level change and its relationship to sequence stratigraphy: rapid depositional rates, tectonic stability, and well-preserved cosmopolitan fossils suitable for age control throughout the time interval of interest (see summary in Miller and Mountain, 1994). In addition, there exists a large set of seismic, well log, and borehole data with which to frame the general geologic setting from the coastal plain across the shelf to the slope and rise (Miller and Mountain, 1994) (Figs. F1, F2).

Geologic setting

The U.S. middle Atlantic margin (New Jersey–Delaware–Maryland) is a classic passive margin. Rifting began in the late Triassic (~230 Ma; Sheridan and Grow, 1988; Withjack et al., 1998), and seafloor spreading commenced by the Callovian (~165 Ma; middle Jurassic). Subsequent tectonics have been dominated by simple thermal subsidence, sediment loading, and flexure (Watts and Steckler, 1979; Reynolds et al., 1991). In the region of the Baltimore Canyon Trough, the Jurassic section is composed of thick (typically 8–12 km) shallow-water limestones and shales. A barrier reef complex fringed the margin until the mid-Cretaceous (Poag, 1985). Accumulation rates were generally low during Late Cretaceous to Paleogene siliciclastic and carbonate deposition (Poag, 1985). A major switch from carbonate ramp deposition to starved siliciclastic sedimentation occurred in the late middle Eocene onshore to earliest Oligocene on the slope in response to global and regional cooling (Miller and Snyder, 1997). Sedimentation rates increased dramatically in the late Oligocene to Miocene (Poag, 1985; Miller and Snyder, 1997). The cause of this large increase is unknown, although it may reflect tectonics in the hinterland (Poag and Sevon, 1989; Sugarman et al., 1993).

Previous drilling

Drilling into the New Jersey slope (ODP Sites 902–904 and 1073) and the Coastal Plain (Island Beach, Atlantic City, Cape May, Bass River, Ancora, Ocean View, Bethany Beach, Millvile, Fort Mott, Sea Girt, and Cape May Zoo) has provided a chronology for sea level events over the past 100 m.y. (Miller et al., 1996a, 1998, 2005a). Sequence boundaries from 10 to 42 Ma defined on the basis of onshore facies successions, erosional criteria, and hiatuses have been shown to correlate (within ±0.5 m.y.) offshore to packages of seismic reflections linked to drill cores on the continental slope and, most importantly, to the history of glacio-eustatic lowerings inferred by the global $\delta^{18}O$ record (Fig. F3). These correlations establish a firm tie between late middle Eocene to middle Miocene glacio-eustatic change and margin erosion on the million year scale. Oxygen isotopic studies of slope Site 904 provide direct evidence for a causal connection between Miocene $\delta^{18}O$ increases (inferred glacio-eustatic falls) and sequence boundaries (Miller, Sugarman, Browning, et al., 1998). Results of these studies are consistent with the general num-

ber and timing of Oligocene to middle Miocene global sequences published by EPR (Vail and Mitchum, 1977; Haq et al., 1987), although amplitudes of the accompanying sea level changes derived by the EPR group are substantially higher than those derived in New Jersey studies (Miller et al., 1996b, 2005a; Miller, Sugarman, Browning, et al., 1998; Van Sickel et al., 2004).

Aided by easier access to older strata than is found downdip/offshore, New Jersey coastal plain drilling (Miller et al., 1994, 1996b; Miller, Sugarman, Browning, et al., 1998) has sampled "greenhouse" (Cretaceous to Eocene) sequences and addressed their relationship to global sea level changes. One surprising result has been the evidence for ice sheets back to a time previously considered to be ice-free: comparing Late Cretaceous to middle Eocene onshore hiatuses/sequence boundaries to the global $\delta^{18}O$ record indicates that small ice sheets (<30 m sea level equivalent) waxed and waned in this supposedly ice-free world (Browning et al., 1996; Miller et al., 1998, 2005a, 2005b).

ODP drilling in the Bahamas (Leg 166 and supplementary platform drilling; Eberli, Swart, Malone, et al., 1997) has also provided a chronology of base-level lowerings in prograding carbonate sequences during similar time periods (Fig. F3). These findings represent complementary and supporting evidence to the New Jersey reports of global sea level change during the Miocene.

These independent data at the New Jersey and Bahamas margins validate the approach outlined by CO-SOD II (Imbrie et al., 1987), a JOIDES Sea Level Workshop (Watkins and Mountain, 1990), and the JOIDES Sea Level Working Group (JOIDES SL-WG, 1992). In particular,

- Both regions show that the age of sequence boundaries on margins can be determined to better than ±0.5 m.y.;

- Both regions have demonstrated the value of the "transect" approach to drilling passive continental margins (arrays of holes spanning onshore, shelf, and slope settings); and

- The siliciclastic New Jersey margin and the carbonate Bahamas margin yield correlatable records of base-level change, as deduced from definitions of the chronostratigraphy of seismically observed stratal discontinuities.

Despite these accomplishments, drilling on the New Jersey margin prior to Expedition 313 has not provided a complete history of sea level change for the Oligocene–Miocene interval. Although sequences tied to regional reflectors were cored and dated on the continental slope (ODP Leg 150; Mountain,

Miller, Blum, et al., 1994), these efforts provided virtually no information about the amplitudes of past sea level change. Likewise, coastal plain drilling (ODP Legs 150X and 174AX; Miller et al., 1994, 1996b; Kominz et al., 2008, and references therein) led to valuable constraints on how high sea level rose during the last 100 m.y. (Fig. F4), but because of their updip locations, sites from these legs provided little information concerning the extremes of sea level lowstands. This was made clear when evidence of a prominent mid-Miocene eustatic fall drilled during ODP Leg 194 (at the Marion Plateau, northeast Australia; John et al., 2004) provided an estimate of 55 ± 15 m versus ~40 m from onshore backstripping (Kominz et al., 2008). This confirmed the suspicion that, because of their updip location, the New Jersey onshore sites do not capture the full range of Miocene sea level change.

Drilling into the Australian margin also had a serious limitation: it was in a dominantly carbonate province without the benefit of prograding, aggrading packages of siliciclastic sequences that record the cyclic nature of sea level rise and fall. All indications from offshore seismic data point to a lengthy and relatively complete record of sea level change in the shallow-shelf sediments of the New Jersey margin, making this an ideal location to take core samples. It has required incremental advances from initial attempts at drilling with the *JOIDES Resolution* on the outer shelf to finally using the *L/B Kayd* to bring this to fruition during Expedition 313.

Site selection

Setting a 173 ton lift boat down on the seafloor requires seabed assessment to establish sediment type, local topography, and proximity to any seafloor artifacts or natural subseafloor anomalies. Data relevant to each of these were collected by several groups with scientific grants from the U.S. National Science Foundation and the U.S. Office of Naval Research (ONR); additional data were acquired by the European Consortium for Ocean Research Drilling (ECORD) Science Operator (ESO) in March–April 2008.

Three multichannel seismic (MCS) surveys have crossed directly over Holes M0027A–M0029A (Fig. F1) (see the site chapters). A reconnaissance grid using a 120 channel, 6 air gun system aboard the R/V *Ewing* in 1990 was the first demonstration that Oligocene–Miocene clinoforms were well developed at this location (Fig. F2); the R/V *Oceanus* returned with 48 channel generator-injector (GI) gun and HiRes equipment in 1995 and collected remarkably improved images of these same features along line 529 (Fig F5). The R/V *Cape Hatteras* used identical HiRes

gear in 1998 to concentrate on three grids of 150–600 m line spacing designed to provide detailed control on clinoform geometries, as well as to meet the guidelines established by the JOIDES Pollution Prevention and Safety Panel (Fulthorpe and Blum, 1992). A Simrad EM1000 swath-bathymetry/acoustic backscatter survey passed over the drill sites during an ONR-supported STRATAFORM study in 1996; Joint Oceanographic Institutions, Inc. (JOI)/United States Science Advisory Committee (USSAC) supported the collection of additional Simrad EM3000 data over each site in June 1999 (J. Goff and N. Driscoll, pers. comm., 1999). Grab samples within a few hundred meters of each site were collected during this same cruise (J. Goff, pers. comm., 1999). These site-assessment data were reviewed by the IODP Environmental Protection and Safety Panel (EPSP) for comment and input, and an evaluation of hazards posed by subsurface gas was completed for ESO by an independent contractor.

Reaching a long-standing goal

The overriding reason to return to the New Jersey margin is that drill cores on the shallow shelf can recover the lowstand sediments that (1) are missing in the coastal plain, (2) have been dated at slope boreholes, and (3) can be tied to the arrangement of composite siliciclastic packages seen in seismic profiles. Continuous coring in Holes M0027A–M0029A can provide estimates of eustatic amplitudes, a testable record of eustatic variations, and an opportunity to evaluate models that predict the nature and distribution of facies in passive margin strata. It is a rewarding accomplishment that goals developed over years of study during the ODP era and later incorporated in the IODP Science Plan have now been realized.

Scientific objectives

1. Provide a testable sedimentary record of eustatic variations

Backstripping is a proven method for extracting amplitudes of global sea level from passive margin records (e.g., Watts and Steckler, 1979). One-dimensional backstripping is a technique that progressively removes the effects of sediment loading (including the effects of compaction) and paleowater depth from basin subsidence. By modeling thermal subsidence on a passive margin, the tectonic portion of subsidence can be assessed and an apparent eustatic estimate obtained (Kominz et al., 1998, 2008; Van Sickel et al., 2004). Backstripping requires knowing

relatively precise ages, paleodepths, and porosities of sediments, and each of these criteria are best obtained from borehole transects; such transects also allow application of two-dimensional backstripping techniques that account for lithospheric flexural effects, increasing the precision of the eustatic estimates (Steckler et al., 1999; Kominz and Pekar, 2001). However, to be confined, the eustatic component obtained from backstripping needs to be tied to sea level records from other margins and those derived from $\delta^{18}O$ estimates.

Drilling in Holes M0027A–M0029A allows us to make precise Oligocene to early middle Miocene apparent eustatic estimates using backstripping as described above. One-dimensional (Kominz et al., 1998; Van Sickel et al., 2004) and two-dimensional (Kominz and Pekar, 2001) backstripping of onshore New Jersey sites has provided preliminary amplitude estimates of 10–60 m for million year–scale variations, but the estimates are incomplete, particularly for the Miocene, because most lowstand deposits are generally not represented (Miller, Sugarman, Browning, et al., 1998; Miller et al., 2005a) (Fig. **F4**). Amplitude estimates derived from $\delta^{18}O$ studies require assumptions about temperature and the sea level/δ_w calibration; although the uncertainties are large, initial eustatic estimates based on $\delta^{18}O$ records are consistent with backstripping results (Fig. **F4**). Holes M0027A–M0029A are precisely located to recover as nearly a complete set of Oligocene–middle Miocene sequences as possible and, through backstripping, provide a much more direct measure of the full range of amplitudes for this time interval.

When we have obtained precise eustatic estimates from Oligocene to lower middle Miocene records in Holes M0027A–M0029A, we will be able to extend our results to older and younger records. Middle Miocene through Holocene sediments record similar clinoform geometries on the middle to outer New Jersey shelf; by applying calibrations of seismic profiles and facies developed as part of this work, we should be able to derive eustatic estimates for the interval 24–14 Ma. In particular, deriving a firm, independent eustatic estimate from margin sediments will

- Allow us to test temperature assumptions needed to make glacio-eustatic estimates from $\delta^{18}O$ records (Figs. **F3, F4**),
- Provide an estimate of the Oligocene–Miocene sea level/δ_w calibration, and
- Evaluate the Pekar (1999) and Pekar et al. (2002) calibration of 0.09‰/10 m (versus 0.11‰/10 m

for the late Pleistocene) that was based on back-stripping an incomplete coastal plain record.

Although both the backstripping and $\delta^{18}O$ methods make inherently large assumptions with inherently large uncertainties, the convergence of the two methods (Fig. F4) suggests that we will be able to produce a testable eustatic model.

2. Test models of sedimentation on siliciclastic shelves

Shallow-water records contain unconformities observed in outcrop or in the subsurface at all spatial scales, whether they divide beds or basins. Unconformably bounded sequences are the fundamental building blocks of the shallow-water record (Sloss, 1963; Van Wagoner et al., 1990; Christie-Blick, 1991). Researchers at the EPR (Vail et al., 1977; Haq et al., 1987; Posamentier et al., 1988; Van Wagoner et al., 1988) claimed that similarities in the ages of stratal unconformities pointed to global sea level (eustasy) as the overriding control. The resulting "eustatic curve" has remained controversial (e.g., Christie-Blick et al., 1990; Miall, 1991), largely because of basic assumptions about the stratigraphic response to eustatic change and because the work relies in part on unpublished data. In response to this controversy, Christie-Blick and Driscoll (1995), among others, pointed out that the fundamental activity of interpreting the origin of layered rocks does not really require any assumptions about eustasy. They emphasized that sequence boundaries attest to changes in depositional base-level. The timing of many of the EPR sequence boundaries has been validated onshore New Jersey and correlated to the $\delta^{18}O$ proxy of eustatic change (Miller et al., 1998, 2005a), although other sequence boundaries on this and other margins may be tectonically derived. Whether or not sequence boundaries are caused by changes in eustasy, local tectonism, or sediment supply (Reynolds et al., 1991), disconformable surfaces irrefutably divide the shallow-water record into sequences. Whatever their cause, these stratal breaks are real and they provide an objective means of analyzing the rock record.

Facies between sequence boundaries vary in a coherent fashion, and various models have been proposed to explain observed spatial and temporal patterns in shelf settings (e.g., Posamentier et al., 1988; Galloway, 1989a, 1989b). Much work has been done by the exploration and academic communities in testing and applying these models, and much has been learned (see Catuneanu et al., 2009). Nonetheless, the complex interaction of processes controlling sequence architecture is not well enough understood for a single model to successfully predict facies successions in all depositional settings.

A major reason that models are poorly constrained and difficult to apply to a variety of settings is that there has been no publicly available study of continuous cores across a prograding siliciclastic clinoform deposit, which constitutes the central element of many facies models. As a result, the water depths in which clinoforms form and the distribution of lithofacies they contain are poorly known. It is widely debated whether clinoform tops ever become subaerially exposed during sea level lowstands and whether the shoreline ever retreats to (or perhaps moves seaward of) the clinoform rollover (Fulthorpe and Austin, 1998; Austin, Christie-Blick, Malone, et al., 1998; Fulthorpe et al., 1999; Steckler, et al., 1999). Settling these controversies will have significant implications on our understanding of how sequence boundaries develop and how much of the facies distribution within clinoforms can be attributed to eustatic variation. Some researchers assume that the shoreline is always located at the clinoform rollover (e.g., Posamentier et al., 1988; Lawrence et al., 1990; Van Wagoner, 1990). Others have presented models that suggest the shoreline and the clinoform rollover move independently of each other (e.g., Steckler et al., 1993, 1999). The sea level estimates of Greenlee and Moore (1988) argue that sea level falls expose an entire continental shelf and that strata onlapping clinoform fronts are coastal plain sediments deposited during the beginning of the subsequent sea level rise. Many researchers (e.g., Steckler et al., 1993) stress that if strata onlapping clinoform fronts were deposited at or near sea level, then the clinoform heights dictate that sea level occasionally fell hundreds of meters in less than a million years; such magnitudes and rates are beyond the reasonable scales of any known mechanism for eustatic change (Pitman and Golovchenko, 1983; Harrison, 1990). Extracting the amplitude of sea level fluctuations from sequence architecture is critically dependent on whether the lowest point of onlap onto sequence boundaries is truly coastal or deeper marine. Determining water depths at the clinoform edge is essential to sequence stratigraphic models and to understanding this basic element of the dynamic land/sea interface. It can only be established by sampling, as done during Expedition 313.

Operational strategy

The region between the paleoshoreline and the paleo-inner to middle shelf is the most sensitive region for studying past sea level variations and was therefore targeted by Expedition 313 to obtain estimates of eustatic amplitudes. Reliability of these estimates depends on the accuracy of two separate measure-

ments: (1) paleowater depths determined by lithologic facies and benthic foraminifer associations and (2) basin response to the spatial and temporal changes in sedimentation. Biofacies associations are generally clearest and paleodepth resolution optimal in nearshore to inner neritic environments (<30 m paleodepth), but unfortunately these associations are difficult to date. Consequently, biologic indicators of paleowater depth are best determined in nearshore to middle neritic facies; they become less precise in facies deeper than middle neritic (>100 m; see examples in Miller and Snyder, 1997). Work onshore New Jersey has shown that the best results can be obtained by targeting sequences deposited between 0 and 60 m paleodepth (Kominz and Pekar, 2001). Basin response is a sum of dewatering/compaction of the underlying sediment, thermal subsidence of the lithosphere, and regional bending of the crust due to the load of deposited sediment. Several of these parameters are insufficiently constrained to provide reliable estimates for sea level calculations if applied to just one location; a transect of sites along which smoothly changing values can be assumed provides the best opportunity for calculating these effects on depositional history. In view of these constraints, and following guidelines developed by a JOIDES Sea Level workshop (Watkins and Mountain, 1990) and the JOIDES Sea Level Working Group (JOIDES SLWG, 1992), the ideal drilling strategy is summarized in Figure F6.

Holes M0027A–M0029A target upper Oligocene to middle Miocene seismically imaged prograding clinoforms that were deposited in inner–middle neritic paleodepths (based on coeval onshore strata deposited in nearshore/prodelta settings). We obtained excellent seismic profiles of these clinoforms at locations that are most likely to record the full amplitude of sea level change: immediately landward of and near the toes of the clinoforms (i.e., across the clinoform inflection point). Modern water depths in Holes M0027A–M0029A are around 34–36 m (Fig. F7), a fortunate "crossover" depth between being too far landward for detailed control on sequence geometry (i.e., thorough seismic control on land is not possible) and too far seaward for affordable commercial drill rigs. Holes M0027A–M0029A were optimally located to sample several clinoform packages across a 22 km transect.

Principal results

Lithostratigraphy

The lithostratigraphic description of sediments cored in Holes M0027A–M0029A on the New Jersey shelf shows that sediments were deposited in two general contexts: (1) mixed storm- and river-dominated shelf with well-sorted silt and sand deposited in offshore to shoreface environments and (2) intrashelf clinoform rollover, clinoform slope, and toe-of-slope settings are dominated by poorly sorted coarse-grained debrites and turbidites with interbedded silt and silty clays. Fine-grained deposits are usually silt-rich and show a notable paucity of clays. The open shelf experienced frequent periods of dysoxia with cyclical repetitions. We found no evidence of exposure at the clinoform rollover (depositional shelf break). However, the periodic occurrences of shoreface facies along the slope of clinoforms and of offshore facies on the topset of the clinoforms in the same seismic sequence suggest large-amplitude changes in relative sea level. All statements below regarding depositional setting are interpretations based on Expedition 313 Science Party core observations. Refer to "Chronology" for refined ages, "Biostratigraphy" for paleodepth estimates, and "Stratigraphic correlation of seismic and sedimentary sequences" for comparison of key stratigraphic surfaces identified in core, well logs, and seismic data.

Hole M0027A

A summary of the lithologic units and major lithologies in Hole M0027A is provided in Figure F8. The lithology at the base of Hole M0027A (Unit VIII) is clay (Unit VIII; 631.15–625.60 meters below seafloor [mbsf]; late Eocene) deposited in a deep offshore environment. The overlying Unit VII (625.60–488.75 mbsf; Oligocene to lowermost Miocene [Aquitanian]) comprises a large-scale coarsening-upward sequence from silt to very fine sand to poorly sorted glauconite-rich coarse sand debrites and turbidites. Cyclic changes in average grain size and glauconite content occur upcore on the scale of 5–10 m; however, sedimentary structures are in places obscured by bioturbation. The succession records the progradation of clinoform slope apron systems over deep (>200 m?) distal clinoform toesets. Unit VI (488.75–355.72 mbsf; upper Aquitanian to lower Burdigalian) marks the outbuilding (progradation) of a thick storm-dominated river-influenced delta (offshore to shoreface) over a toe-of-slope apron. A thick shoreface succession (Subunit VIA; ~57 m thick) comprises clean quartz sand. The overlying Unit V (355.72–335.93 mbsf; lower mid-Burdigalian) marks an abrupt change in lithofacies and mineralogy to poorly sorted glauconite-rich sands with quartz and lithic granules whose environment of deposition in a clinoform rollover position is poorly constrained. Univ IV (335.93–295.01 mbsf; mid-Burdigalian) comprises a deepening-upward shoreface–offshore transition to offshore succession lacking a regressive

facies. An erosional surface separates lithostratigraphic Units IV and III (295.01 mbsf), which begins with ~1.5 m of very coarse glauconitic sand representing a condensed transgressive lag deposit. Unit III (295.01–236.16 mbsf; upper Burdigalian to lower Langhian) is composed of deepening- and shallowing-upward packages of silty offshore and shoreface–offshore transition environments with a major storm influence. Unit II (236.16–167.74 mbsf; Langhian) consists of a series of fining- and deepening-upward sedimentary cycles that are interpreted as transgressive shoreface evolving to shoreface–offshore transition deposits. These cycles are thought to be incomplete depositional sequences from which regressive facies successions have been subsequently eroded. The upper part of Unit II consists of a clay-rich offshore succession. Unit I (167.74–0 mbsf; upper Miocene and upper Pleistocene, with no identified Pliocene) comprises sands and gravels deposited in a range of fluvial, coastal plain, estuarine, shoreface, and incised valley environments.

Hole M0028A

A summary of the lithologic units and major lithologies in Hole M0028A is provided in Figure F9. The oldest stratigraphic unit in Hole M0028A (Unit VII; 668.66–662.98 mbsf; mid-upper Aquitanian) comprises dark brown siltstone with thin-walled articulated shells deposited in a low-energy deep offshore environment. Unit VI (662.98–611.19 mbsf; Aquitanian to lowermost Burdigalian[?]) is a pale brown clayey silt with intercalated very fine and fine sand beds representing a river-dominated offshore (prodelta) environment. The contact with overlying Unit V (611.19–525.52 mbsf; lower Burdigalian) is abrupt and bioturbated. Unit V is divided into three subunits of poorly sorted coarse-grained gravity flow deposits. The poorly sorted coarse sediments are interpreted as deposits from high-concentration flows at the toe of slope of a degraded clinothem. Subunits VB and VC are dominated by debrites and Subunit VA by turbidites. Unit IV (525.52–512.29 mbsf; mid-Burdigalian) consists of sediment gravity flows, possibly from river flood events, deposited in an offshore environment. Unit III (512.29–335.37 mbsf; mid–upper Burdigalian) is divided into four subunits that mark the shallowing-upward and outbuilding of a storm-dominated river-influenced delta. Subunit IIID consists of toe-of-clinoform apron deposits of coarse sand with gravel abruptly overlying silts from Unit IV. Subunits IIIB and IIIC contain interbedded silts and two-part sands, interpreted as storm flows deposited in a shoreface–offshore transition setting. Poorly recovered Subunit IIIA comprises clean quartz sandstone deposited in a shoreface setting. Unit II

(335.37–223.33 mbsf; upper Burdigalian to lower Serravalian[?]) is also divided into four subunits that mark a series of offshore to shoreface cycles. Subunit IID is poorly sorted and dominantly coarse grained, with a mix of mud, coarse sand, and gravel deposited at a clinoform rollover. The position may be gully fills and/or small deltas. These sediments fine uphole into offshore silts. A sharp contact separates Subunit IID from Subunit IIC, which consists of shoreface–offshore transition deposits. The succession initially fines and then gradually coarsens uphole from clay and silt to medium sand, indicating a transition from an offshore to a river-influenced shoreface–offshore transition setting. Contact with Subunit IIB is characterized by in situ glauconite in an offshore setting. The overlying intervals of poorly sorted quartzose gravelly sandstone are high-concentration sediment gravity flow deposits within a channelized environment. The fining then coarsening of the overlying succession reveals a deepening then shallowing from offshore to shoreface–offshore transition settings. The contact between Subunits IIB and IIA is marked by an abrupt grain-size break separating poorly sorted coarse sand with granules (below) from clayey silt (above). In Subunit IIA, an erosional surface that cuts into offshore silts with rare storm event beds is overlain by coarse to fine sand with bored nodules and glauconite grains, indicating condensed deposition (hiatus) followed by seafloor erosion and exhumation, which is overlain again by clay in an offshore environment. Unit I was not cored in Hole M0028A.

Hole M0029A

A summary of the lithologic units and major lithologies in Hole M0029A is provided in Figure F10. Unit VII (756.33–747.27 mbsf; lower Oligocene to lower Miocene) consists of siltstone with glauconite sand and thin-walled articulated shells deposited in a low-energy deep offshore environment. Unit VI (747.27–728.55 mbsf; late Aquitanian to early Burdigalian) is a pale brown clayey silt with intercalated very fine and fine sands deposited in a river-dominated offshore (prodelta) setting. Units V through III (728.55–640.51 mbsf; middle early Miocene to early middle Miocene) contain a series of granuliferous quartz and glauconite coarse sand packages separated by bioturbated silts. Sands are generally sharp based and often grade uphole into silts. Sands are interpreted to represent toe-of-clinoform-slope apron systems deposited during lowered sea level and silts to represent deep offshore sediments deposited during high sea level. Subunit IID (640.51–602.25 mbsf) contains two packages of poorly sorted glauconitic medium to coarse sand overlain by bioturbated silt. The deposi-

tional environment was toe-of-clinoform-slope apron at base and deep offshore on top.

Unit II (640.51–325.12 mbsf; middle Miocene [Langhian]) is divided into several subunits. Sediments in Subunit IIC (602.33–502.01 mbsf), comprising a monotonous succession of very fine sandy silt and silt, were deposited in a deep offshore environment below storm wave base. Subunit IIB (502.01–448.49 mbsf) contains three sediment packages. The two packages at the base coarsen uphole from medium to coarse sand grading to silt. The upper package contains poorly sorted slightly shelly silt with gravels. These sediments likely represent sediment gravity flow deposition on a clinoform slope, either within a submarine channel or intraslope apron environment. Subunit IIA (448.49–325.12 mbsf) is another monotonous very fine sandy silt and silt with rare sandier units. These represent offshore river-influenced offshore environments. Unit I (325.12–3.85 mbsf; upper Serravalian[?] and upper Pleistocene) was spot-cored to identify major reflectors. Sediments recovered were likely deposited in a range of shelf settings, from shallow marine shoreface to foreshore, coastal plain, and estuarine environments.

Biostratigraphy

Study of the fossils found in Holes M0027A, M0028A, and M0029A provides important constraints on the age, paleoenvironment, and paleowater depth of sediments deposited on the New Jersey shallow shelf. Age assignments based on calcareous nannofossils, planktonic foraminifers, and dinocysts are in generally good agreement (Figs. F11, F12, F13), although they do show some evidence of diachrony of biostratigraphic markers across unconformities between Holes M0027A and M0029A. Calcareous microfossils are more abundant and more consistently present downhole, allowing for better age control at the more distal Hole M0029A. Benthic foraminifer biofacies indicate paleobathymetric changes within a sequence stratigraphic and lithologic framework, including both shallowing-upward and deepening-upward successions. Pollen studies identified a hemlock horizon across all three holes, indicating the presence of temperate forests and humid conditions on the Atlantic coastal plain during the early Miocene (early Burdigalian). Middle Miocene pollen assemblages record the expansion of grasses and sedges, indicating increasing aridity at that time. The main results for the three drilled holes follow.

Hole M0027A

Pleistocene, Miocene, Oligocene, and possible uppermost Eocene sections were identified from calcareous nannofossils, planktonic foraminifers, and dinocysts (Fig. F11) and integrated with Sr isotope stratigraphy to establish a chronostratigraphic framework for Hole M0027A (Fig. F14). There is generally good agreement between the biohorizons of the different microfossil groups and the Sr isotope ages in this hole. The exception is within the Oligocene section; calcareous nannofossils indicate an expanded upper Oligocene section, whereas dinocysts do not.

The abundance and preservation of calcareous microfossils and dinocysts varies significantly throughout the hole, with barren intervals coinciding with coarse-grained sediments in the Miocene and younger sections. The prevalence of sands, particularly in the middle Miocene, may have resulted in depressed biostratigraphic last occurrences, particularly within the calcareous microfossils. Reworking of Paleogene material also made biostratigraphy challenging, predominantly within the lower Miocene sediments.

Paleobathymetry and paleoenvironments determined from benthic foraminifers, dinocysts, and terrigenous palynomorphs show that paleodepths varied throughout Hole M0027A, ranging from inner neritic (0–50 m) to outer neritic (100–200 m). Paleobathymetric fluctuations indicate shallowing- and deepening-upward trends that correlate with the evolution of depositional environments. In general, lithofacies and benthic foraminifer biofacies correlate well. Similarly, benthic foraminifer water depth estimates and palynological estimates of proximity to shoreline are consistent. Palynological data support previous reconstructions of a warm, humid early Neogene climate during the Eocene–Oligocene transition and early Neogene, whereas the Oligocene witnessed intervals of drier and cooler conditions, causing the spread of herbal taxa and conifer forests.

Hole M0028A

Middle and lower Miocene sections were identified from calcareous nannofossils, planktonic foraminifers, and dinocysts (Fig. F12) and integrated with Sr isotope stratigraphy to establish a chronostratigraphic framework for Hole M0028A (Fig. F14). Abundant reworking of Paleogene material made assigning ages to some intervals difficult, but there is generally good agreement between the planktonic microfossil groups and ages based on Sr isotopes. As in Hole M0027A, barren intervals coincide with

coarse-grained sediments, diminishing biostratigraphic age control within intervals of the lower Miocene.

Paleodepths vary through the Miocene section of Hole M0028A, ranging from inner to middle neritic (0–100 m). In several sequences, paleobathymetric fluctuations indicate shallowing-upward successions. In general, lithostratigraphic units and benthic foraminifer biofacies correlate well. Similarly, benthic foraminifer water depth estimates and palynological estimates of proximity to shoreline are consistent. Palynological data support previous reconstructions of a warm, humid early Neogene climate.

Hole M0029A

Pleistocene and middle and lower Miocene sections were identified from calcareous nannofossils, planktonic foraminifers, and dinocysts (Fig. F13) and integrated with Sr isotope stratigraphy to establish a chronostratigraphic framework for Hole M0029A (Fig. F14). There is generally good agreement among the ages obtained from the different planktonic microfossil groups, which is particularly important in this hole because the Sr isotope ages within the middle Miocene strata have substantial scatter. Microfossils are also more abundant in this hole, allowing for age refinements within the lower Miocene sections that are barren of planktonic microfossils in the previous holes. As in the previous holes, reworked Paleogene material occurs throughout the Miocene sections, although it is more concentrated in the lower Miocene, making age assignments somewhat difficult in certain intervals.

Paleobathymetric estimates for Hole M0029A are based on benthic foraminifer occurrences, which indicate that paleodepths fluctuated from the outer neritic zone (100–200 m) to the inner neritic zone (0–50 m). Benthic foraminifer biofacies changes indicate that paleobathymetric fluctuations occur within a sequence stratigraphic framework, with several sequences showing a shallowing-upward succession and one showing a deepening-upward succession. Benthic foraminifer water depth estimates and palynological estimates of proximity to the shoreline show excellent agreement. As with the previous holes, palynological data support reconstructions of a warm, humid early Neogene climate.

Paleomagnetism

The main objective of the shore-based paleomagnetic studies was to produce a polarity magnetostratigraphy in as much detail as possible within the time constraints of the Onshore Science Party. At se-

lected depth intervals for all three holes, attempts were also made to characterize the remanence carrier and to make preliminary estimates of relative paleointensity. These objectives were achieved through measurements of natural remanent magnetization (NRM) and alternating-field (AF) demagnetization of discrete samples taken from Expedition 313 cores.

Sediments from Holes M0027A–M0029A generally possess a weak or unstable NRM. However, clay-rich horizons in all holes exhibit much stronger magnetic moments, accompanied by peaks in magnetic susceptibility. AF demagnetization up to 15–30 mT, depending on lithology, typically removes a low-coercivity overprint with normal polarity, sometimes revealing a higher coercivity stable component. Inclination data show prevailing normal polarity, suggesting that the first component is a viscous overprint. In Hole M0028A, the inclination data also showed frequent reversals carried by stable components. When compared to the general age-depth constraints, it is suspected that either the normal or reversed parts of the interval in question (Cores 313-M0028A-7R and 8R) were caused by a chemical remanent magnetization (CRM). During AF demagnetization a few samples acquired what was identified as gyroremanent magnetization (GRM). The effect of GRM was removed by applying an anti-gyroremanent demagnetization procedure.

Two reversal boundaries were successfully identified in Hole M0027A within the clay sequence in upper Unit II and could be assigned to either C5ACn or C5ADn, based on age constraints from Sr and biostratigraphic analyses. In Hole M0028A, a polarity magnetization could only be established for two intervals from ~223 to 255 mbsf and ~610 to 669 mbsf. Within these intervals, six reversal boundaries were identified: C5ABr or C5ACr (between 242.30 and 242.59 mbsf), C5AAn or C5ABn (between 226.23 and 226.53 mbsf), C6Ar (between 665.91 and 666.41 mbsf), C6An.2n (between 655.92 and 656 34 mbsf), C6An.1r (between 622.65 and 622.90 mbsf), and C6An.1n (between 616.52 and 617.02 mbsf). In Hole M0029A, five boundaries were tentatively identified: C5Aar (between 331.11 and 330.91 mbsf), C5AAn (between 327.95 and 327.53 mbsf), C5Acn through C5ADN (thick zone of normal polarity between 370 and 470 mbsf), C6An.1r (between 733.29 and 733.49 mbsf), and part of all of C6An.2n (~747 mbsf).

Magnetic mineral dissolution was observed in thin section and may explain, in part, the weak NRM of these sediments. Additionally, authigenic magnetic minerals associated with glauconite pellets were identified in thin section, explaining the observed

relationship between high magnetic susceptibility and glauconite-bearing sediments.

Petrophysics and logging

Petrophysical and downhole log data collected during Expedition 313 are essential for correlation between sedimentological observations and seismic interpretations, thus aiding our understanding of the sequence stratigraphy of the New Jersey margin.

Offshore, the petrophysics program included wireline logging and collection of high-resolution, nondestructive measurements on whole cores using the Geotek multisensor core logger (gamma density, transverse compressional wave velocity, electrical resistivity, and magnetic susceptibility). A graphical summary of the downhole measurements made during Expedition 313 is given in Figure F15.

Onshore, the petrophysics program involved measuring natural gamma radiation (NGR) and thermal conductivity (TC) on whole cores, split-core digital line scan imaging, and split-core color reflectance. Lower resolution measurements on discrete samples for *P*-wave velocities and moisture and density were also performed. Some petrophysical and downhole measurements display variation primarily with depositional sedimentary changes, whereas some are controlled by other factors such as the degree of post-depositional cementation or diagenesis and the type of interstitial water.

For all three holes, preliminary results from the petrophysics and logging program are of a methodological character. These data enable correlation of sedimentologic observations, downhole logs, and seismic reflections, thereby providing the backbone for sequence stratigraphic interpretations. The continuity and quality of the downhole through-pipe gamma log data in all three holes is especially valuable, particularly in intervals where no core was obtained. There is excellent correlation between all open-hole logs with the through-pipe gamma ray logs, both in depth and in correlation of distinctive features. Repeat sections of open-hole spectral gamma were collected in Hole M0027 to provide a comparison and calibration to the through-pipe spectral gamma ray data. This led to a very high level of confidence in using the continuous through-pipe gamma as a basis for stratigraphic correlations between holes. Furthermore, natural gamma ray (NGR) measurements on the unsplit cores will enable an even higher degree of core-log-seismic correlation by providing precise core depth positioning with respect to log depth.

Where NGR measurements were not distinctive, other logs, notably magnetic susceptibility, were found to be useful for core-log correlation. Magnetic susceptibility can be matched to line scan images and can indicate mineral variation at a high resolution (e.g., darker layers showing increased magnetic susceptibility related to minerals associated with pyritization). Also, the magnetic susceptibility in conjunction with the K/Th ratio is an excellent detector of glauconite, a mineral thought to indicate dysoxic, sediment-starved conditions.

Downhole acoustic images acquired during Expedition 313 are a useful tool for identifying important sequence stratigraphic surfaces in the intervals where they were collected (Fig. F15). The highest resolution images were obtained from a 30 m section from Hole M0028A. Images from digital line scanning proved very helpful in detecting sedimentological changes, enabling reliable comparison of features observed in the core with the in situ images of the borehole wall.

Information from the sonic velocity logs and gamma-derived density logs provide a basis for identifying impedance contrasts. These data sets give insight into both lithology and potential seismic reflectors and will aid interpretation of the sequences. Two high-quality sections of sonic velocity data were acquired in Hole M0027A (Fig. F15) and one section in Hole M0029A.

Changes in density and porosity very closely match lithology changes (grain size and mineral content). Overall, the porosity of specific grain size ranges (clay, silt, and sand) decrease exponentially with burial depth. Anomalously low porosity in the upper ~200 m of Holes M0027A and M0029A is tentatively related to the coring technique. In general, large-scale coarsening-upward sequences and abrupt decreases in grain size can be recognized by changes in density and porosity (as well as gamma ray).

Interesting links between the geochemical results and petrophysical data were identified, as highlighted by the conductivity logs and resistivity data on the core. Electrical conductivity trends are mainly controlled by the chlorinity of the pore fluids in Holes M0027A, M0028A, and the upper part of Hole M0029A (Figs. F8, F9, F10). In contrast, although both conductivity and chlorinity values are high in Hole M0029A, especially chlorinity below 320 mbsf, lithology controls the numerous electrical conductivity variations in Hole M0029A. In all holes, except in the lower part of Hole M0029A, the highest chlorinities are generally correlated with a low gamma ray signal indicative of coarse-grained formations.

In Hole M0029A, particularly distinct conductivity, sonic, and magnetic susceptibility values clearly identified boundaries between lithologic units. This

was especially valuable in the several instances where boundaries occurred in a coring gap. This also occurred in some intervals in Holes M0027A and M0028A.

Interstitial water chemistry

A total of 222 interstitial water samples were taken from the cores using Rhizon samplers and by squeezing, and 179 sediment samples for analysis of headspace gas were collected offshore. We measured pH, alkalinity, salinity, and ammonium in the interstitial water onboard. Chlorinity in these waters was measured by electrochemical titration at the University of Hawaii in June and July 2009. With the assistance of the technical staff at the University of Bremen, we measured an additional 17 chemical species in the interstitial water, including chloride, bromide, and sulfate by ion chromatography and Li, Na, K, Mg, Ca, Sr, Ba, Mn, Fe, B, Al, Si, P, and S by inductively coupled plasma–atomic emission spectrometry (ICP-AES). We also analyzed the sediment for total C and S, total organic carbon, and mineralogy by X-ray diffraction.

The upper several hundred meters of sediment beneath the continental shelf off New Jersey is dominated by freshwater interlayered with saltwater of nearly seawater chlorinity in all three holes. These layers may be correlatable from hole to hole. At greater depths the chloride concentration increases to seawater value in Hole M0027A and to higher concentrations in the other two holes. In Hole M0029A, brine is encountered toward the bottom of the hole. Although fresh to saltwater chemistry dominates, the waters have reacted with sediment and these reactions are in part microbially mediated.

Hole M0027A

The salient characteristics of interstitial water from Hole M0027A are how fresh it is and how frequently and abruptly it alternates from fresh to salty downhole. The upper part of the hole (to 419 mbsf) contains five distinct layers of relatively fresh water, some thin and some thick, which alternate with salty layers and are separated from them by sharp gradients in chloride concentration (Fig. F8). The mean chloride concentration in the hole is 273 mM, indicating that overall nearly half of the pore water in Hole M0027A is fresh. A central task in interpreting the pore water chemistry is to explain how these sharp salinity gradients are maintained in the face of chemical diffusion, which tends to soften such gradients and then, over time, erase them altogether. Both the fresh and saltwater layers have distinct chemistries that may enable us to correlate them from hole to hole. Below the deepest fresh layer chloride in-

creases linearly to its concentration in seawater while, relative to chloride, Na, K, and B decrease and Li, Mg, and Sr increase. Br and Ca show no large net change. Sulfate is reduced to low concentrations by microbial oxidation of organic matter, causing alkalinity, ammonium, and Ba to increase and holding Ca steady by precipitation of $CaCO_3$. The largest anomaly in pore water composition, of unknown origin, occurs at 394 mbsf as a large peak in Mn, Fe, Si, B, Li, K, Ca, and Sr, corresponding with the lowest Na/Cl ratio measured in the hole.

Hole M0028A

Like Hole M0027A, the pore water chemistry of Hole M0028A is dominated by the alternation of relatively fresh and salty layers (Fig. F9). Although we did not core the upper part of the hole, the shallowest sample recovered, from 225 mbsf, has only 14% of the chloride content of seawater. Below that depth there are at least two additional layers of fresher water alternating with saltier layers. Neglecting the brine near the bottom of the hole at 627–664 mbsf, the mean chloride concentration is 309 mM, indicating that overall ~40% of the pore water in the hole is fresh. Although the mean water is not as fresh as that in Hole M0027A, relatively fresh water extends to a greater depth, 536 mbsf. Below that depth, salinity increases until the water becomes a brine, with 608 mM chloride. Microbes appear to have been much more successful in reducing sulfate within the fresher water layers than within the saltier ones, in the process of oxidizing organic matter in the sediment, as the fresher layers have <1 mM sulfate and very low sulfate/chloride ratios, whereas the intervening saltier layers have values typical of seawater. As in Hole M0027A, the major fresh and saltwater layers appear to have distinct chemistries. These chemistries and the unique shapes of some of the depth profiles, particularly for chloride and sulfate, are proving useful for correlating the various fresher and saltier layers between Holes M0027A and M0028A.

Hole M0029A

Like Holes M0027A and M0028A, Hole M0029A displays alternating layers of fresher and saltier water within the upper 300 m of the hole, including the lowest chloride concentration we measured in any of the holes, 19 mM (Fig. F10). Unlike the earlier holes, Hole M0029A contains an increasingly saline brine from 345 mbsf to the deepest sample at 748 mbsf, which reaches 995 mM, nearly twice the concentration of seawater. This brine appears to be similar to that encountered at several holes drilled on the upper to mid-slope during Leg 150. For the depth inter-

val above the brine, the mean chloride concentration is 314 mM, nearly identical to the 309 mM in Hole M0028A, indicating that overall ~40% of the pore water is fresh. The fresher layers again appear to have distinct, perhaps unique, compositions. Relative to the chloride concentration in seawater, the brine is depleted in Na, K, Mg, and sulfate and enriched in Br, Li, B, Ca, Sr, Fe, alkalinity, and ammonium.

Stratigraphic correlation of seismic and sedimentary sequences

A primary objective of Expedition 313 is to tie seismic sequences to cores and logs. Depths of seismic sequence boundaries (identified by onlap, downlap, and erosional truncation of reflectors on a regional seismic grid) were calculated at each site using a velocity-depth function derived from stacking velocities that had been used to process these same profiles. We examined cores and/or logs at these calculated depths (Fig. F16), and in the following section we discuss the extent of agreement between these "predictions" and the actual lithologic or log expression of demonstrably disconformable surfaces. Several additional unconformities not recognized on seismic data were found in the cores (three in Hole M0027A and three in Hole M0029A). Furthermore, three flooding surfaces were also identified in Hole M0029A that had no apparent seismic expression. By contrast, some seismic features could not be attributed to a single surface in the cores, but rather to a set of distinct yet closely spaced lithologic discontinuities that were either sequence boundaries, surfaces of transgression, or maximum flooding surfaces. Minor inconsistencies between seismic and sedimentologic features in cores and on MSCL and downhole logs are probably due to inaccuracies in the time-depth function that would be sampled at downdip locations in subsequent holes.

Hole M0027A

Hole M0027A provided the first test of tying seismic sequence boundaries to cores, logs, and age control. The site was chosen to enable us to sample seismic sequences updip of clinoform rollovers, while at the same location sample older sequences downdip of their clinoform rollovers landward of this hole.

There were insufficient data in nearby wells to guide our estimates of where the base of the Pleistocene section would be at any of the Expedition 313 sites. Slight angular discordance in shallow reflectors in MCS line 529 crossing Hole M0027A suggested the base of the Pleistocene would be at roughly 36 mbsf. The deepest occurrence of Pleistocene nannofossils and the top of a thick interval of fluvial/estuarine

sediments barren of microfossils suggests this disconformable Pleistocene/Miocene contact is more likely at 32 mbsf. Studies using higher resolution Geopulse profiles (Sheridan et al., 2000) placed the base of the Pleistocene at roughly 36 mbsf if the time-depth conversion used in this present study is applied.

Discontinuous coring in the upper Miocene succession (32 to roughly 200 mbsf) made it unlikely that we would recover sediments exactly straddling sequence boundaries m1 and m3. Time-depth calculations predicted these surfaces would be at 91 and 108 mbsf, respectively. We detected a downhole decrease in gamma ray values at about 96 m and another at 115 mbsf, and we tied these to seismic events m1 and m3, respectively. The first of these, m1, matches the base of a paleosol, whereas m3 matches the top of a ~55 m interval of fluvial/estuarine sand.

Calculated depths of seismic sequence boundaries m4.5, m5.2, m5.3, m5.32, m5.45, m5.6, and m5.7 match remarkably well (within 1–7 m; i.e., better than ±3%) with lithologic features consistent with depositional sequence boundaries. The calculated depth of seismic sequence boundary m5.47 most closely matches a flooding surface but occurs within 4 m of a facies change interpreted to be a depositional sequence boundary. Seismic sequence boundary m5.7 coincides with a gamma log kick, whereas we link seismic sequence boundary m5.8 to a lithologic sequence boundary that is ~10 m deeper than the calculated depth. The calculated depth of seismic sequence boundary m6 has no definite equivalent in the core, and its precise placement is uncertain, though it is expected to mark a major (>1 m.y.) hiatus. The depth of reflector o.5 (not mapped in the existing seismic grid) was predicted at 540–545 m. There is no immediately recognizable log or lithofacies feature that is reasonably close to this depth. However, there is a 4 m.y. hiatus implied at 540 mbsf by Samples 313-M0027A-191R-CC (late Oligocene, Zone DN1) and 192R-CC (middle Oligocene >28 Ma). Reflector o1 is associated with an impedance contrast (see Fig. F69 in the "Site M0027" chapter) and a minor lithologic break (see Fig. F81 in the "Site M0027" chapter). Three other Oligocene surfaces noted in the cores appear to be sequence boundaries with significant hiatuses but are below seismic resolution.

Hole M0028A

Hole M0028A is located 12 km downdip from Hole M0027A. Seismic sequences that had been sampled along their topsets in Hole M0027A were targets for sampling in Hole M0028A near their clinoform rollovers. Older sequences in Hole M0027A that were sampled at clinoform slopes would be sampled at

this site in a toeset setting. In this way, Holes M0027A and M0028A provide the opportunity to test models of depositional sequence development by sampling sequences at several key locations.

The upper 220 m in Hole M0028A was drilled without coring. The first seismic features sampled were two previously unnamed reflectors. The calculated depth of the first, m4.1, corresponds to a maximum flooding surface and several small but closely spaced high density values; the calculated depth of the second, m4.5, matches a significant downhole increase in impedance generated predominantly by a sharp increase in density measured by the MCSL.

Calculations predict seismic sequence boundary m5 is between 258 and 263 mbsf. No obvious feature was observed in log data at this depth or in the corresponding cores, but core recovery was unusually poor in this exact interval. The most likely feature we detected is the base of a quartz sand interval at 269 mbsf. Seismic sequence boundary m5 marks a change in seismic facies: the ~15 m interval above is acoustically transparent, and immediately below m5 there are several closely spaced, subparallel reflectors.

The calculated depth of seismic sequence boundary m5.2 is exactly the depth of the lower of two closely spaced impedance contrasts due to sharp density increases (see Fig. F56 in the "Site M0028" chapter). The lower surface has the lithofacies character of a flooding surface; 2 m above it, the other is interpreted as a depositional sequence boundary.

It is difficult to match surfaces in the core with sequence boundaries m5.3, m5.32, and m5.33 because of incomplete core recovery. The calculated depth of seismic boundary m5.4 is associated with a sharp impedance contrast at 495 mbsf (see Fig. F66 in the "Site M0028" chapter). It lies at the base of a very thick coarsening-upward succession and is consistent with the interpretation of a depositional sequence boundary. The calculated depth of seismic sequence boundary m5.45 likewise matches a lithologic expression of a sequence boundary and a sharp impedance contrast; the core expression of m5.47 appears to be ~5 m shallower than the calculated depth of the seismic event.

The calculated depth for seismic sequence boundary m5.6 closely matches the sedimentary discontinuity placed in a coring gap that corresponds to a significant downhole decrease in gamma ray values and coincident sharp decrease in impedance. The core surface associated with seismic sequence boundary m5.7 (predicted depth of 589–599 mbsf) is uncertain. However, three surfaces are noted in the core

between 600 and 610 mbsf, and the reflection may be a response to one or more of these features.

The lithologic expression of seismic sequence boundary m5.8 is placed 9 m deeper than the calculated depth. We find the most reasonable match to be at a major burrowed contact separating silty glauconite sand above from sandy siltstone below that matches a large and sharp downhole decrease in density.

Hole M0029A

Drilling in Hole M0029A completed the program designed to sample individual clinoforms at three different positions: at the clinoform rollover, in topset beds landward of that position, and seaward of that position in toeset beds. Hole M0029A sampled the thickest section of middle Miocene found during Expedition 313, and seismic data showed that two previously unnamed seismic unconformities within the middle Miocene would be sampled.

Seismic correlations to locally high gamma ray log values in Holes M0027A and M0028A were traced to Hole M0029A, and these depths guided offshore attempts to spot core similar facies in the upper 256 m. Several surfaces in estuarine, fluvial, and possible paleosol sediments were recovered, and the calculated depths of seismic reflectors m1, m3, and m4 in Hole M0029A match sharp changes in the gamma ray logs. There was insufficient time during the Onshore Sampling Party (OSP) to narrow the range of any uncertainties in these links.

Continuous coring began at 256 mbsf, and, as expected, we found that the calculated depths of seismic reflectors matched flooding surfaces in cores more often in this hole than in the other two. This was true for reflectors m4.1, m4.3, and m4.4, whereas the calculated depth for m4.2 correlates to a sedimentary unconformity marked also by a major kick in bulk density and a minimum in the gamma ray values. Calculated depths of seismic reflectors m4.5 and m5 occur at very sharp, localized highs in MSCL density values and major impedance contrasts (see Fig. F53 in the "Site M0029" chapter). The predicted depth of seismic reflector m5.2 corresponds fairly well (there is a 6 m, or roughly 1%, discrepancy) to a sequence boundary described in the core and a major impedance contrast.

Because of the downdip location of Hole M0029A, the sequences below m5.2 are significantly thinner than they are in the other two holes. Combined with the subdued lithologic contrasts between sequences, this fact led to uncertain seismic-core correlations because of the overlapping error ranges of depth cal-

culations (a few percent of total depth) and the subtle petrophysical features that generate the seismic reflections. Consequently, at this stage in our analysis there are several possible seismic-core correlations for reflectors m5.3, m5.4, m5.45, and m5.47. The predicted depth of reflector m5.6 occurs in a coring gap that correlates to a significant peak in gamma ray values due to high K concentrations; a major impedance contrast occurs across this gap (see Fig. F63 in the "Site M0029" chapter). We match a surface to reflector m5.7 that is ~10 m shallower than the calculated depth. However, the sedimentological expression of this discontinuity is an obvious and major lithologic break between siltstone with glauconite sand overlying pale brown clayey silt. It is unclear whether Hole M0029A penetrated seismic sequence boundary m5.8. There are several possible placements, including two major coring gaps. The upper one at the peak of gamma ray values, corresponding to glauconitic clays, is higher than the predicted depth. Two other possible horizons match well the predicted depths but lie in coring gaps. Only the refinement of biostratigraphy, core, and seismic correlations can clarify whether this seismic surface was penetrated and if so at what position in the core.

Chronology

Expedition 313 chronology for the uppermost Eocene? to Pleistocene sections is based on integrating biostratigraphy and Sr isotopic ages obtained in Holes M0027A, M0028A, and M0029A (Fig. F14). Below we describe preliminary age assignments of depositional sequences, each named by the seismic sequence boundary tentatively correlated to the base of each depositional unit as described in the previous section of this report.

Hole M0027A

The uppermost sequence above 10 mbsf is upper Pleistocene (<90 ka), one or more underlying Pleistocene sequences occur between 90 and 250 ka, and there is a thin lower Pleistocene sequence (~1 m.y.; 26–32 mbsf). No ages are available for sequences m1, m3, and m4 at this location. Reflector m4.1 is interpreted as a maximum flooding surface that cannot be resolved on profiles from three older surfaces (m4.2, m4.3, and m4.4, dated in Hole M0029A) and must represent a significant hiatus that is not discernible with the available age control. A series of relatively thin (<25 m) sequences (m5.2, an unnamed sequence, 5.3, 5.32, 5.4, and yet another unnamed sequence) span the lower/middle Miocene boundary (16.2 Ma). Preliminary ages for these sequences appear to be younger than in Holes M0028A and M0029A, which we attribute to depressed last

occurrences of biostratigraphic markers in this updip sandy hole. Sequences m5.4, an unnamed sequence (295 mbsf), m5.45, and m5.47 have basal age estimates ranging from ~17.3 to 18.4 Ma but have fairly large errors because of limited data. Future work should improve the age estimates. A 37 m thick m5.45 sequence and a thin m5.47 sequence are estimated as ~18.0 and ~18.3 Ma, respectively, and are reasonably well constrained with a ±0.5 m.y. age resolution. Thin sequences m5.6 and m5.7 have no current calcareous nannofossil–derived age constraint (barren/non–age diagnostic nannofossils) except superposition, although they contain shells and further analyses are expected to produce ages based on dinocysts and Sr isotopes. A thick (128.1 m) m5.8 sequence has a lower boundary dated as 21.1 Ma. A thin lowermost Miocene sequence (m6) is dated only by assignment to mid–calcareous nannofossil Zone NN2 (~21–21.5 Ma).

The Oligocene succession is substantially thicker (>129 m) than has previously been found onshore, and there are five Oligocene sequences and part of an uppermost Eocene(?) to lowermost Oligocene sequence based on lithofacies. The uppermost Oligocene sequence is poorly dated at present. The o1 sequence is well dated by all fossil groups and Sr isotopes as mid-Oligocene (28.5–29.0 Ma) and may link well to astronomical predictions of insolation. Two underlying Oligocene sequences are poorly dated. The lowermost Oligocene sequence is assigned to lower Oligocene calcareous nannofossil Zone NP22 (23.46–32.8 Ma), whereas the base of the hole is in lower Zone NP21 (>32.8 Ma) based on the common occurrence of *Ericsonia formosa,* suggesting that Chron C13n and some of upper Chron C13r (the Eocene/Oligocene boundary) is represented by a hiatus across a sequence boundary.

Hole M0028A

Chronology for the middle to lower Miocene section in Hole M0028A is based on integrating biostratigraphy and Sr isotopic ages. The upper Miocene to Pleistocene was not cored. Sequence m4.5 is moderately well constrained to ~13–15 Ma by Sr isotopes (13.8 Ma ± 1.17 m.y.), calcareous nannofossil Zones ?NN6 and NN5 (12.6–15.6 Ma), planktonic foraminifer Zone N10/M7 (12.7–14.8 Ma), and foraminifer datum levels. Sequence m5 is constrained by Sr isotopes (14.0 Ma ± 1.17 m.y.) and dynocyst Zones DN5 (13.2–15.2 Ma) and NN5 (13.6–15.6 Ma) to yield a preliminary age of ~14–15.2 Ma. Sequence m5.2 is constrained by Sr isotopes (~16 Ma ± 0.8 m.y.) and Zones DN4 (15.2–16.8 Ma), NN5, and NN4 (15.2–16.8 Ma). The NN4/NN5 zonal boundary provides a firm age constraint (15.6 Ma) within the sequence.

Sequence m5.3 is constrained in age by the combination of Sr isotopes (16.5 Ma ± 0.6 m.y.), Zone NN4 (15.6–18.2 Ma), and Zone DN2–DN3 (16.8–22.0 Ma) to yield an age estimate of 16–17 Ma and a possible basal age of ~16.6 Ma. Sequence m5.4 is assigned to Zones NN4, N6/M3 (17.3–18.8 Ma) or older, and DN3 (16.8–19.2 Ma) and Sr isotope ages of ~17 Ma ± 0.8 m.y., with a basal age of 17.3–18.3 Ma. Sequence m5.45 is assigned to Zones NN4 (<18.42 Ma) and DN2–DN4 and Sr isotope ages of 18.6 Ma ± 0.6 m.y. The base of the sequence is clearly younger than 18.4 Ma but could be as young as ~17 Ma with a best estimate of ~18.2 Ma. Sequence m5.47 has little age constraint other than superposition. Sequence m5.6 is only constrained by the presence of *Globorotalia praescitula* (<18.5 Ma) and the presence of Zone NN4 (<18.42 Ma) at the top. Sequence m5.7 has no constraints other than superposition (18.6 to ~20.5 Ma). Sequence m5.8 is assigned to mid-Zone NN2 (~20–21.5 Ma) and Zone DN2 (19.2–22.0 Ma). Provisional magnetostratigraphy identifies a thick (>18 m) normal magnetozone in the lower part of this sequence that may be Chron C6AN.2n, suggesting a basal age of ~21.5 Ma. Sequence m6 was just penetrated at the bottom of the hole, with an Sr isotope age of 20.7 Ma ± 0.6 m.y.

Sedimentation rates before decompaction are difficult to estimate with certainty in Hole M0028A based on these preliminary age constraints. Typical sedimentation rates are 40 m/m.y. Sedimentation rates during deposition of the targeted m5.4 sequence in a position near its greatest thickness were ~100–145 m/m.y.

Hole M0029A

The Pleistocene to upper middle Miocene section was spot-cored in Hole M0029A, and the hole bottomed in the lower Miocene. In general, age control at this site is better than at the updip locations. Calcareous nannofossils suggest that the uppermost sequence (above 14 mbsf) is upper Pleistocene (Zone NN21; <250 ka). There are no other age constraints on ?Pleistocene sequences and seismic sequence boundaries m1, m3, and m4 in Hole M0029A. Seismic sequence m4.2 is poorly dated. It is assigned to calcareous nannofossil Zones NN6 (12.6–13.2 Ma) and NN6–NN7, dinocyst Zones DN6–DN8 (younger than ~13.2 Ma), and planktonic foraminifer Zone N14 or older (>11.4 Ma), with scattered Sr isotope ages yielding an average of 12.8 Ma ± 0.8 m.y. The underlying tentative sequence termed m4.5 is assigned to dinocyst Zones DN6–DN8 (<13.2 Ma) and DN5 (13.2–15.1 Ma), nannofossil Zones NN6 (11.8–13.6 Ma) and NN5 (13.6–15.6 Ma), a foraminifer datum level of ~13.8 Ma, and Sr isotope ages of 13.8 Ma ± 0.7 m.y., yielding an age of ~13.5–14.6 Ma for the

sequence. Sequence m5 is assigned to Zones NN5 (13.6–15.6 Ma) and DN5 (13.2–15.1 Ma), together with a foraminifer datum level of 14.8 Ma and Sr isotope ages of 14.2 Ma ± 0.8 m.y.; this yields an age assignment of 14.6–15.4 Ma, with a possible basal age of 15.0–15.4 Ma. The age of sequence m5.2 is well constrained as 15.6–16.1/16.2 Ma by biostratigraphy (Zones NN4 and NN5, DN4–DN5, and N8/M5). The finding of the Zone NN4/NN5 boundary (15.6 Ma) in the middle of this sequence both in this hole and in Hole M0028A contrasts with its placement within sequence m5.3 in Hole M0027A, suggesting a depressed last occurrence in the updip site. The age of seismic sequence m5.3 is constrained to Zones NN4 (15.6–18.2 Ma) and upper Zones DN3–DN4 and a Sr isotope age of 16.9 Ma ± 0.6 m.y.; its basal age is estimated as ~16.2–16.9 Ma. The ages of sequences m5.4, m5.45, and m5.47 cannot be precisely estimated because they are assigned to the long Zone NN4 (<18.2 Ma) and dinocyst Zone DN3 or older (>16.7 Ma). There are no current Sr isotope age estimates, but subsequent work should constrain the ages of these sequences. Sequence m5.6 has reasonable age constraints in Hole M0029A versus the updip sites. Here, for the first time, Zone NN3 (18.3–19.6 Ma) was identified, remarkably consistent with an Sr isotope age of 18.3 Ma ± 0.6 m.y. Sequence m5.7 is assigned to the middle part of calcareous nannofossil Zone NN2 (19.6–21.5 Ma and Zone DN2 (19 to ~20.2 Ma), with a best estimate of 19.6–20.2 Ma. Sequence m5.8 is assigned to the mid-upper part of Zone NN2 (older than 19.6 and younger than 21.5 Ma) and Zone DN2 (19– 22.2 Ma). It has a Sr isotope age estimate of 21.0 Ma ± 0.6 m.y., suggesting that the sequence is 20.4–21.6 Ma. We may have drilled through sequence boundary m5.8 and into the underlying sequence m6. Dinocysts suggest that the base of Hole M0029A was in Zone DN1 (>22.2 Ma). However, nannofossils suggest that the base of Hole M0029A was younger than 21.5 Ma, remarkably consistent with an Sr isotope age of 21.3 Ma ± 0.6 m.y. These ages are more consistent with assignment to sequence m5.8 based on regional correlations.

Sedimentation rates before decompaction are difficult to estimate in Hole M0029A from the preliminary age constraints. Typical sedimentation rates are ~80 m/m.y. Sedimentation rates during deposition of the targeted m5.2 sequence in a position near its greatest thickness were ~176 m/m.y.

Preliminary scientific assessment and conclusions

The two overarching goals of Expedition 313 were to (1) recover a complete and measurable record of Oligocene–Miocene eustatic variation and (2) evaluate

models of sedimentation on siliciclastic continental shelves during a time of known eustatic oscillations. Achieving both goals will require considerable shore-based analysis and integration among disciplines, and it is too early to gauge how successful we will be. Nonetheless, there are several positive indications, among which are the following.

Target section recovered

- Despite penetrating the Miocene/Oligocene boundary in only Hole M0027A, the key target interval of middle to early Miocene was cored in all three holes with 80% recovery.

- Core quality is in general very good to excellent; poorly lithified sand was a drilling and coring challenge in the post–middle Miocene section above roughly 200 mbsf at all holes, as well as in several older intervals (sometimes several tens of meters thick) in Holes M0027A and M0028A.

- The value of a drilling transect strategy was demonstrated by the many thin (10–20 m) topset units drilled in one or both of Holes M0027A and M0028A that could be matched by age, facies, log, and/or seismic correlation to the toeset strata seaward of clinoform rollovers.

Good geochronologic control

- An additional purpose of drilling a transect of holes was to improve the chance of more nearly continuous accumulation in a basinward, deeper setting than is found in the more landward, shallower holes; initial geochronology shows this has worked exactly as planned.

- Mollusk fragments and benthic foraminifers have thus far provided >100 $^{87}Sr/^{86}Sr$ age dates.

- Calcareous nannofossils are often abundant and provide ages largely consistent with Sr isotope ages.

- Dinocysts and pollen prepared prior to the OSP are common in many intervals, and additional studies will be beneficial; the presence of distinctive pollen assemblages restricted in time are present in all three holes, potentially providing narrow and unexpected correlation markers.

- Shore-based preparation of planktonic foraminifers showed they are common in some intervals, and post-OSP analysis will provide additional age control.

- Although additional demagnetization of low-susceptibility sediments is required to measure remanent inclination values, certain fine-grained intervals have shown that magnetochronology will assist in our final age control.

Reliable paleobathymetric indicators

- Benthic foraminifer assemblages are found in fine-grained intervals in each hole, providing an indication of water depths (relative sea levels) at the time of deposition.

- Thanks to excellent core quality, primary sedimentary structures (e.g., low-angle cross-bedding indicating a shoreface environment, storm beds preserved as fining-upward sharp-based sands, etc.) provide an independent measure of paleobathymetry.

- Vertical facies successions across surfaces and within sequences yield trends in paleodepths that provide broad-scale indicators of depositional environments and suggest a range of sediment transport mechanisms.

Extensive physical measurements

- Gamma ray response was logged through the pipe for 98% of the 2065 m of drilled hole, vertical seismic profiles were acquired in 83%, and a combination of five logging tools deployed in open hole covered roughly 46% of the entire drilled section; these data provide properties of the sediment and pore fluids even in the ~20% of the cored intervals not recovered.

- The MSCL provided continuous measurements of core properties and core-wireline log correlation to confirm accurate ties between these data.

- Excellent quality seismic reflection images provide stratal geometry that, with accurately depth-registered physical characteristics from logs and MCSL data, will lead to confident seismic-core correlation.

These results suggest we will be able to date the lower to middle Miocene section with accuracy sufficient to compare breaks in the record with times of sea level lowering predicted by the ages of $\delta^{18}O$ glacio-eustatic proxy. We are confident we will be able to match these breaks to seismic sequence boundaries that have been traced to drill holes dated on the slope and to the shoreline where extrapolation to sediments in the modern coastal plain have also been dated in drill holes. We already know we have recovered sediment (mostly in our most basinward Hole M0029A) not found previously in the coastal plain, presumably because of nondeposition/erosion during times of sea level lowstand at those updip locations. Dating and matching sediments to the seismic record is only part of the objective; incorporating estimates of paleobathymetry, compaction history, and basin subsidence will be needed to backstrip this transect and arrive at estimates for the magnitude of eustatic (global) sea level change. This task

lies ahead, but for now we know we have datable, nearly continuously deposited sediment of the right age to compare to a sea level proxy. Furthermore, we will have the ability to build on (1) excellent core quality and continuity, (2) firm core-log-seismic integration, and (3) a transect across several clinoforms in developing a model of siliciclastic successions during a time of known large eustatic variations.

Offshore operations

Expedition 313 carried three types of coring tools: a hydraulic piston corer (HPC; equivalent to the advanced piston corer [APC]), an extended nose corer (EXN; equivalent to the extended core barrel [XCB]), and a standard rotary corer (ALN; equivalent to the rotary core barrel [RCB]). See Table **T1** for a summary of operations. Please see the **"Methods"** chapter for a description of the coring technology.

Onshore Science Party, Bremen

The cores and samples collected offshore New Jersey were transported under refrigeration to the IODP Bremen Core Repository and Laboratories in the MARUM building on the campus of Bremen University (Germany). Frozen microbiology samples were forwarded from Bremen to scientists' laboratories in Germany and France by special courier service. NGR logging and thermal conductivity measurements were acquired before the start of the OSP (see the **"Methods"** chapter). Further analytical laboratories were accessed by agreement with the Department of Geosciences (geochemistry, paleomagnetics, mineralogy [X-ray diffraction], and hydrofluoric acid laboratories) and the Center for Marine Environmental Sciences (MARUM) (physical properties, micropaleontology, and nondestructive core logging laboratories) at Bremen University.

During the Expedition 313 Onshore Science Party (6 November–4 December 2009), the cores were described in detail and minimum and some standard measurements were made (Table **T2**). In addition, sampling for postcruise scientific research was also undertaken.

References

Austin, J.A., Jr., Christie-Blick, N., Malone, M.J., et al., 1998. *Proc. ODP, Init. Repts.,* 174A: College Station, TX (Ocean Drilling Program). **doi:10.2973/ odp.proc.ir.174a.1998**

Backman, J., Moran, K., McInroy, D.B., Mayer, L.A., and the Expedition 302 Scientists, 2006. *Proc. IODP,* 302: Edinburgh (Integrated Ocean Drilling Program Management International, Inc.). **doi:10.2204/ iodp.proc.302.2006**

Bartek, L.R., Vail, P.R., Anderson, J.B., Emmet, P.A., and Wu, S., 1991. Effect of Cenozoic ice sheet fluctuations in Antarctica on the stratigraphic signature of the Neogene. *J. Geophys. Res., [Solid Earth],* 96(B4):6753–6778. **doi:10.1029/90JB02528**

Berggren, W.A., Kent, D.V., Swisher, C.C., III, and Aubry, M.-P., 1995. A revised Cenozoic geochronology and chronostratigraphy. *In* Berggren, W.A., Kent, D.V., Aubry, M.-P., and Hardenbol, J. (Eds.), *Geochronology, Time Scales and Global Stratigraphic Correlation.* Spec. Publ.—SEPM (Soc. Sediment. Geol.), 54:129–212.

Berggren, W.A., and Pearson, P. N., 2005. A revised tropical to subtropical Paleogene planktonic foraminiferal zonation. *J. Foraminiferal Res.,* 35(4):279–298. **doi:10.2113/ 35.4.279**

Browning, J.V., Miller, K.G., McLaughlin, P.P., Kominz, M.A., Sugarman, P.J., Monteverde, D., Feigenson, M.D., and Hernández, J.C., 2006. Quantification of the effects of eustasy, subsidence, and sediment supply on Miocene sequences, mid-Atlantic margin of the United States. *Geol. Soc. Am. Bull.,* 118(5):567–588. **doi:10.1130/B25551.1**

Browning, J.V., Miller, K.G., and Pak, D.K., 1996. Global implications of lower to middle Eocene sequence boundaries on the New Jersey Coastal Plain: the icehouse cometh. *Geology,* 24(7):639–642. **doi:10.1130/ 0091-7613(1996)024<0639:GIOLTM>2.3.CO;2**

Camoin, G.F., Iryu, Y., McInroy, D.B., and the Expedition 310 Scientists, 2007. *Proc. IODP,* 310: Washington, DC (Integrated Ocean Drilling Program Management International, Inc.). **doi:10.2204/iodp.proc.310.2007**

Cande, S.C., and Kent, D.V., 1995. Revised calibration of the geomagnetic polarity timescale for the Late Cretaceous and Cenozoic. *J. Geophys. Res.,* 100(B4):6093–6095. **doi:10.1029/94JB03098**

Catuneanu, O., Abreu, V., Bhattacharya, J.P., Blum, M.D., Dalrymple, R.W., Eriksson, P.G., Fielding, C.R., Fisher, W.L., Galloway, W.E., Gibling, M.R., Giles, K.A., Holbrook, J.M., Jordan, R., Kendall, C.G.St.C., Macurda, B., Martinsen, O.J., Miall, A.D., Neal, J.E., Nummedal, D., Pomar, L., Posamentier, H.W., Pratt, B.R., Sarg, J.F., Shanley, K.W., Steel, R.J., Strasser, A., Tucker, M.E., and Winker, C., 2009. Towards the standardization of sequence stratigraphy. *Earth-Sci. Rev.,* 92(1–2):1–33. **doi:10.1016/j.earscirev.2008.10.003**

Cazenave, A., Dominh, K., Guinehut, S., Berthier, E., Llovel, W., Ramillien, G., Ablain, M., and Larnicol, G., 2009. Sea level budget over 2003–2008: a reevaluation from GRACE space gravimetry, satellite altimetry and Argo. *Global Planet. Change,* 65(1–2):83–88. **doi:10.1016/j.gloplacha.2008.10.004**

Christie-Blick, N., 1991. Onlap, offlap, and the origin of unconformity-bounded depositional sequences. *Mar. Geol.,* 97(1–2):35–56. **doi:10.1016/0025-3227(91)90018-Y**

Christie-Blick, N., and Driscoll, N.W., 1995. Sequence stratigraphy. *Annu. Rev. Earth Planet. Sci.,* 23(1):451–478. **doi:10.1146/annurev.ea.23.050195.002315**

Christie-Blick, N., Mountain, G.S., and Miller, K.G., 1990. Seismic stratigraphic record of sea-level change. *In* National Research Council (Ed.), *Sea-level Change:* Washington, DC (National Academy Press), 116–140.

Church, J.A., and White, N.J., 2006. A 20th century acceleration in global sea level rise. *Geophys. Res. Lett.,* 33(1):L01602. doi:10.1029/2005GL024826

de Verteuil, L., and Norris, G., 1996. Miocene dinoflagellate stratigraphy and systematics of Maryland and Virginia. *Micropaleontology,* 42 (Suppl.). doi:10.2307/1485926

Donovan, D.T., Jones, E.J.W., Ridd, M.F., and Hubbard, J.A.E.B., 1979. Causes of world-wide changes in sea level, with discussion. *J. Geol. Soc. (London, U. K.),* 136(2):187–193. doi:10.1144/gsjgs.136.2.0187

Eberli, G.P., Swart, P.K., Malone, M.J., et al., 1997. *Proc. ODP, Init. Repts.,* 166: College Station, TX (Ocean Drilling Program). doi:10.2973/odp.proc.ir.166.1997

Embry, A., 2008–2009. Practical sequence stratigraphy. *Reservoir,* 35(5)–36(8).

Fairbanks, R.G., 1989. A 17,000-year glacio-eustatic sea level record: influence of glacial melting rates on the Younger Dryas event and deep-ocean circulation. *Nature (London, U. K.),* 342(6250):637–642. doi:10.1038/342637a0

Fairbanks, R.G., and Matthews, R.K., 1978. The marine oxygen isotope record in Pleistocene coral, Barbados, West Indies. *Quat. Res.,* 10(2):181–196. doi:10.1016/0033-5894(78)90100-X

Fulthorpe, C.S., and Austin, J.A., Jr., 1998. Anatomy of rapid margin progradation: three-dimensional geometries of Miocene clinoforms, New Jersey margin. *AAPG Bull.,* 82(2):251–273.

Fulthorpe, C.S., Austin, J.A., Jr., and Mountain, G.S., 1999. Buried fluvial channels off New Jersey: did sea-level lowstands expose the entire shelf during the Miocene? *Geology,* 27(3):203–206. doi:10.1130/0091-7613(1999)027<0203:BFCONJ>2.3.CO;2

Fulthorpe, C.S., and Blum, P. (Eds.), 1992. Ocean Drilling Program guidelines for pollution prevention and safety. *JOIDES J.,* 18(7). http://www.odplegacy.org/PDF/Admin/JOIDES_Journal/JJ_1992_V18_No7.pdf

Galloway, W.E., 1989a. Genetic stratigraphic sequences in basin analysis, I. Architecture and genesis of flooding-surface bounded depositional units. *AAPG Bull.,* 73(2):125–142.

Galloway, W.E., 1989b. Genetic stratigraphy sequences in basin analysis, II. Application to northwest Gulf of Mexico Cenozoic Basin. *AAPG Bull.,* 73(2):143–154.

Greenlee, S.M., and Moore, T.C., 1988. Recognition and interpretation of depositional sequences and calculation of sea-level changes from stratigraphic data—offshore New Jersey and Alabama Tertiary. *In* Wilgus, C.K., Hastings, B.S., Posamentier, H., Van Wagoner, J.C., Ross, C.A., and Kendall, C.G.St.C. (Eds.), *Sea-level Changes: An Integrated Approach.* Spec. Publ.—Soc. Econ. Paleontol. Mineral., 42:329–353.

Haq, B.U., Hardenbol, J., and Vail, P. R., 1987. Chronology of fluctuating sea levels since the Triassic. *Science,* 235(4793):1156–1167. doi:10.1126/science.235.4793.1156

Harrison, C.G.A., 1990. Long-term eustasy and epeirogeny in continents. *In* National Research Council (Ed.), *Sea-Level Change:* Washington, DC (Natl. Acad. Press), 141–158.

Imbrie, J., Barron, E.J., Berger, W.H., Bornhold, B.D., Cita Sironi, M.B., Dieter-Haass, L., Elderfield, H., Fischer, A., Lancelot, Y., Prell, W.L., Togweiler, J.R., and Van Hinte, J., 1987. Scientific goals of an Ocean Drilling Program designed to investigate changes in the global environment. In *Report of the Second Conference on Scientific Ocean Drilling (COSOD II):* Strasbourg (European Science Foundation), 15–36.

John, C.M., Karner, G.D., and Mutti, M., 2004. δ^{18}O and Marion Plateau backstripping; combining two approaches to constrain late middle Miocene eustatic amplitude. *Geology,* 32(9):829–832. doi:10.1130/G20580.1

JOIDES SL-WG, 1992. Sea Level Working Group. *JOIDES J.,* 18(3):28–36. http://www.odplegacy.org/PDF/Admin/JOIDES_Journal/JJ_1992_V18_No3.pdf

Katz, M.E., Wright, J.D., Miller, K.G., Cramer, B.S., Fennel, K., and Falkowski, P.G., 2005. Biological overprint of the geological carbon cycle. *Mar. Geol.,* 217(3–4)323–338. doi:10.1016/j.margeo.2004.08.005

Kinoshita, M., Tobin, H., Ashi, J., Kimura, G., Lallemant, S., Screaton, E.J., Curewitz, D., Masago, H., Moe, K.T., and the Expedition 314/315/316 Scientists, 2009. *Proc. IODP,* 314/315/316: Washington, DC (Integrated Ocean Drilling Program Management International, Inc.). doi:10.2204/iodp.proc.314315316.2009

Kominz, M.A., Browning, J.V., Miller, K.G., Sugarman, P.J., Misintseva, S., and Scotese, C.R., 2008. Late Cretaceous to Miocene sea-level estimates from the New Jersey and Delaware coastal plain coreholes: an error analysis. *Basin Res.,* 20(2):211–226. doi:10.1111/j.1365-2117.2008.00354.x

Kominz, M.A., Miller, K.G., and Browning, J.V., 1998. Long-term and short-term global Cenozoic sea-level estimates. *Geology,* 26(4):311–314. doi:10.1130/0091-7613(1998)026<0311:LTASTG>2.3.CO;2

Kominz, M.A., and Pekar, S.F., 2001. Oligocene eustasy from two-dimensional sequence stratigraphic backstripping. *Geol. Soc. Am. Bull.,* 113(3):291–304. doi:10.1130/0016-7606(2001)113<0291:OEFTDS>2.0.CO;2

Lawrence, D.T., Doyle, M., and Aigner, T., 1990. Stratigraphic simulation of sedimentary basins: concepts and calibration. *AAPG Bull.,* 74(3):273–295.

Martini, E., 1971. Standard Tertiary and Quaternary calcareous nannoplankton zonation. *In* Farinacci, A. (Ed.), *Proc. 2nd Int. Conf. Planktonic Microfossils Roma:* Rome (Ed. Tecnosci.), 2:739–785.

Miall, A.D., 1991. Stratigraphic sequences and their chronostratigraphic correlation. *J. Sediment. Res.,* 61(4):497–505.

Miller, K.G., et al., 1994. *Proc. ODP, Init. Repts.,* 150X: College Station, TX (Ocean Drilling Program). doi:10.2973/odp.proc.ir.150X.1994

Miller, K.G., Kominz, M.A., Browning, J.V., Wright, J.D., Mountain, G.S., Katz, M.E., Sugarman, P.J., Cramer, B.S., Christie-Blick, N., and Pekar, S.F., 2005a. The Phanerozoic record of global sea-level change. *Science,* 310(5752):1293–1298. doi:10.1126/science.1116412

Miller, K.G., Liu, C., Browning, J.V., Pekar, S.F., Sugarman, P.J., Van Fossen, M.C., Mullikin, L., Queen, D., Feigenson, M.D., Aubry, M.-P., Burckle, L.D., Powars, D., and Heibel, T., 1996a. Cape May site report. *Proc. ODP, Init. Repts.,* 150X (Suppl.): College Station, TX (Ocean Drilling Program), 5–28. doi:10.2973/odp.proc.ir.150XS.014.1996

Miller, K.G., and Mountain, G.S., 1994. Global sea-level change and the New Jersey margin. *In* Mountain, G.S., Miller, K.G., Blum, P., et al., *Proc. ODP, Init. Repts.,* 150: College Station, TX (Ocean Drilling Program), 11–20. doi:10.2973/odp.proc.ir.150.102.1994

Miller, K.G., Mountain, G.S., Browning, J.V., Kominz, M., Sugarman, P.J., Christie-Blick, N., Katz, M.E., and Wright, J.D., 1998. Cenozoic global sea level, sequences, and the New Jersey transect: results from coastal plain and continental slope drilling. *Rev. Geophys.,* 36(4):569–602. doi:10.1029/98RG01624

Miller, K.G., Mountain, G.S., the Leg 150 Shipboard Party, and Members of the New Jersey Coastal Plain Drilling Project, 1996b. Drilling and dating New Jersey Oligocene–Miocene sequences: ice volume, global sea level, and Exxon records. *Science,* 271(5252):1092–1095. doi:10.1126/science.271.5252.1092

Miller, K.G., and Snyder, S.W. (Eds.), 1997. *Proc. ODP, Sci. Results,* 150X: College Station, TX (Ocean Drilling Program). doi:10.2973/odp.proc.sr.150X.1997

Miller, K.G., Sugarman, P.J., Browning, J.V., et al., 1998. *Proc. ODP, Init. Repts.,* 174AX: College Station, TX (Ocean Drilling Program). doi:10.2973/odp.proc.ir.174AX.1998

Miller, K.G., Wright, J.D., and Browning, J.V., 2005b. Visions of ice sheets in a greenhouse world. *In* de la Rocha, C.L., and Paytan, A. (Eds.), *Ocean Chemistry over the Phanerozoic and its Links to Geological Processes.* Mar. Geol., 217(3–4):215–231. doi:10.1016/j.margeo.2005.02.007

Miller, K.G., Wright, J.D., and Fairbanks, R.G., 1991. Unlocking the ice house: Oligocene–Miocene oxygen isotopes, eustasy, and margin erosion. *J. Geophys. Res.,* 96(B4):6829–6848. doi:10.1029/90JB02015

Mountain, G.S., Miller, K.G., Blum, P., et al., 1994. *Proc. ODP, Init. Repts.,* 150: College Station, TX (Ocean Drilling Program). doi:10.2973/odp.proc.ir.150.1994

Neal, J., and Abreu, V., 2009. Sequence stratigraphy hierarchy and the accommodation succession method. *Geology,* 37(9):779–782. doi:10.1130/G25722A.1

Pekar, S., 1999. Extracting an eustatic record from the western equatorial Pacific δ^{18}O records and onshore New Jersey Oligocene sequence stratigraphy [Ph.D. thesis]. Rutgers Univ., Piscataway, NJ.

Pekar, S.F., Christie-Blick, N., Kominz, M.A., and Miller, K.G., 2002. Calibration between eustatic estimates from backstripping and oxygen isotopic records for the Oli-
gocene. *Geology,* 30(10):903–906. doi:10.1130/0091-7613(2002)030<0903:CBEEFB>2.0.CO;2

Pitman, W.C., III, and Golovchenko, X., 1983. The effect of sea level change on the shelf edge and slope of passive margins. *Spec. Publ.—Soc. Econ. Paleontol. Mineral.,* 33:41–58.

Poag, C.W., 1985. Depositional history and stratigraphic reference section for central Baltimore Canyon trough. *In* Poag, C.W. (Ed.), *Geologic Evolution of the United States Atlantic Margin:* New York (Van Nostrand Reinhold), 217–264.

Poag, C.W., and Sevon, W.D., 1989. A record of Appalachian denudation in postrift Mesozoic and Cenozoic sedimentary deposits of the U.S. middle Atlantic continental margin. *Geomorphology,* 2(1–3):119–157. doi:10.1016/0169-555X(89)90009-3

Posamentier, H.W., Jervey, M.T., and Vail, P.R., 1988. Eustatic controls on clastic deposition, I. Conceptual framework. *In* Wilgus, C.K., Hastings, B.S., Ross, C.A., Posamentier, H.W., Van Wagoner, J., and Kendall, C.G.St.C. (Eds.), *Sea-Level Changes: An Integrated Approach.* Spec. Publ.—Soc. Econ. Paleontol. Mineral., 42:109–124.

Quinn, T.M., and Mountain, G.S., 2000. Shallow water science and ocean drilling face challenges. *Eos, Trans. Am. Geophys. Union,* 81(35):397. (Abstract) doi:10.1029/00EO00293

Reynolds, D.J., Steckler, M.S., and Coakley, B.J., 1991. The role of the sediment load in sequence stratigraphy: the influence of flexural isostasy and compaction. *J. Geophys. Res., [Solid Earth],* 96(B4):6931–6949. doi:10.1029/90JB01914

Saffer, D., McNeill, L., Araki, E., Byrne, T., Eguchi, N., Toczko, S., Takahashi, K., and the Expedition 319 Scientists, 2009. NanTroSEIZE Stage 2: NanTroSEIZE riser/riserless observatory. *IODP Prel. Rept.,* 319. doi:10.2204/iodp.pr.319.2009

Sheridan, R.E., Ashley, G.M., Miller, K.G., Waldner, J.S., Hall, D.W., and Uptegrove, J., 2000. Offshore-onshore correlation of upper Pleistocene strata, New Jersey coastal plain to continental shelf and slope. *Sediment. Geol.,* 134(1–2):197–207. doi:10.1016/S0037-0738(00)00020-8

Sheridan, R.E., and Grow, J.A., 1988. *The Atlantic Continental Margin: U.S.:* Boulder, CO (Geol. Soc. Am.), Geol. of North Am. Ser., I-2.

Sloss, L.L., 1963. Sequences in the cratonic interior of North America. *Geol. Soc. Am. Bull.,* 74(2):93–114. doi:10.1130/0016-7606(1963)74[93:SITCIO]2.0.CO;2

Stanford, J., Rohling, E.J., Hunter, S.E., Roberts, A.P., Rasmussen, S.O., Bard, E., McManus, J., and Fairbanks, R.G., 2006. Timing of meltwater pulse 1a and climate responses to meltwater injections. *Paleoceanography,* 21(4):PA4103. doi:10.1029/2006PA001340

Steckler, M.S., Mountain, G.S., Miller, K.G., and Christie-Blick, N., 1999. Reconstruction of Tertiary progradation and clinoform development on the New Jersey passive margin by 2-D backstripping. *Mar. Geol.,* 154(1–4):399–420. doi:10.1016/S0025-3227(98)00126-1

Steckler, M.S., Reynolds, D.J., Coakley, B.J., Swift, B.A., and Jarrard, R., 1993. Modelling passive margin sequence stratigraphy. *In* Posamentier, H.W., Summerhayes, C.P., Haq, B.U., and Allen, G.P. (Eds.), *Sequence Stratigraphy and Facies Associations*. Spec. Publ.—SEPM (Soc. Sediment. Geol.), 18:19–41.

Sugarman, P.J., Miller, K.G., Browning, J.V., Kulpecz., A.A., McLaughlin, P.P., Jr., and Monteverde, D.H., 2006. Hydrostratigraphy of the New Jersey coastal plain: sequences and facies predict continuity of aquifers and confining units. *Stratigraphy,* 2(3):259–275.

Sugarman, P.J., Miller, K.G., Owens, J.P., and Feigenson, M.D., 1993. Strontium-isotope and sequence stratigraphy of the Miocene Kirkwood Formation, southern New Jersey. *Geol. Soc. Am. Bull.,* 105(4):423–436. doi:10.1130/0016-7606(1993)105<0423:SIASSO>2.3.CO;2

Underwood, M.B., Saito, S., Kubo, Y., and the Expedition 322 Scientists, 2009. NanTroSEIZE Stage 2: subduction inputs. *IODP Prel. Rept.,* 322. doi:10.2204/iodp.pr.322.2009

Vail, P.R., and Mitchum, R.M., Jr., 1977. Seismic stratigraphy and global changes of sea level, Part 1. Overview. *In* Payton, C.E. (Ed.), *Seismic Stratigraphy: Applications to Hydrocarbon Exploration*. AAPG Mem., 26:51–52.

Vail, P.R., Mitchum, R.M., Jr., and Thompson, S., III, 1977. Seismic stratigraphy and global changes of sea level, Part 2. The depositional sequence as a basic unit for stratigraphic analysis. *In* Payton, C.E. (Ed.), *Seismic Stratigraphy: Applications to Hydrocarbon Exploration*. AAPG Mem., 26:53–62.

Van Sickel, W.A., Kominz, M.A., Miller, K.G., and Browning, J.V., 2004. Late Cretaceous and Cenozoic sea-level estimates: backstripping analysis of borehole data, onshore New Jersey. *Basin Res.,* 16(4):451–465. doi:10.1111/j.1365-2117.2004.00242.x

Van Wagoner, J.C., Mitchum, R.M., Campion, K.M., and Rahmanian, V.D., 1990. *Siliciclastic Sequence Stratigraphy in Well Logs, Cores, and Outcrops: Concepts for High-Resolution Correlation of Time and Facies*. AAPG Methods Explor., 7.

Van Wagoner, J.C., Posamentier, H.W., Mitchum, R.M., Jr., Vail, P.R., Sarg, J.F., Loutit, T.S., and Hardenbol, J., 1988. An overview of the fundamentals of sequence stratigraphy and key definitions. *In* Wilgus, C.K., Hastings, B.S., Ross, C.A., Posamentier, H.W., Van Wagoner, J., and Kendall, C.G.St.C. (Eds.), *Sea-Level Changes: An Integrated Approach*. Spec. Publ.—Soc. Econ. Paleontol. Mineral., 42:39–45.

Watkins, J.S., and Mountain, G.S. (Eds.), 1990. *Role of ODP Drilling in the Investigation of Global Changes in Sea Level*. Rep. JOI/USSAC Workshop, El Paso, TX, Oct. 24–26, 1988.

Watts, A.B., and Steckler, M.S., 1979. Subsidence and eustasy at the continental margin of eastern North America. *In* Talwani, M., Hay, W., and Ryan, W.B.F. (Eds.), *Deep Drilling Results in the Atlantic Ocean: Continental Margins and Paleoenvironment*. Maurice Ewing Ser., 3:218–234.

Withjack, M.O., Schlische, R.W., and Olsen, P.E., 1998. Diachronous rifting, drifting, and inversion on the passive margin of eastern North America: an analogue for other passive margins. *AAPG Bull.,* 82(5A):817–835. http://aapgbull.geoscienceworld.org/cgi/content/abstract/82/5A/817

Figure F1. The New Jersey continental margin showing Holes M0027A, M0028A, and M0029A along with other completed boreholes both onshore and offshore. Tracks of reconnaissance seismic lines relevant to the goals of Expedition 313 are also shown. MAT = Mid-Atlantic Transect, ODP = Ocean Drilling Program, DSDP = Deep Sea Drilling Project.
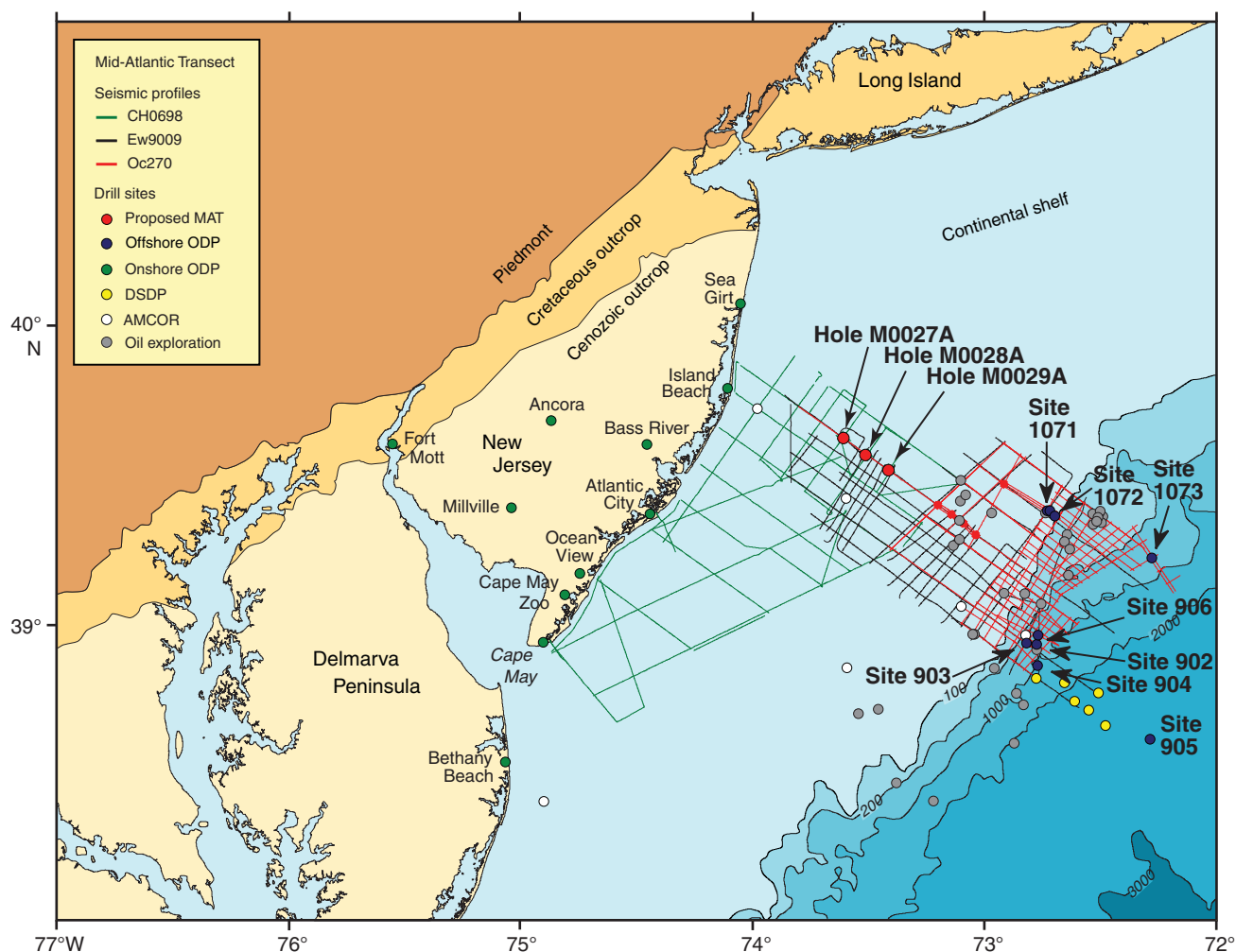
Figure F2. Ew9009 line 1003 through Holes M0027A, M0028A, and M0029A (yellow subseafloor columns; see Fig. F1 for location). Generalized locations of ODP boreholes onshore and offshore (gray columns) and previously proposed but undrilled Sites MAT-4A to MAT-7A (white columns) are also shown. Several key surfaces (colored lines; K/T boundary = ~65 Ma, o1 = ~33.5 Ma, m5 = ~16.5 Ma, m4 = ~14 Ma, m3 = ~13.5 Ma, and m1 = ~11.5 Ma) have been traced from the inner shelf to the slope. The clinoform shape of sediments bracketed by these unconformities is thought to be the result of large sea level fluctuations (Vail and Mitchum, 1977).
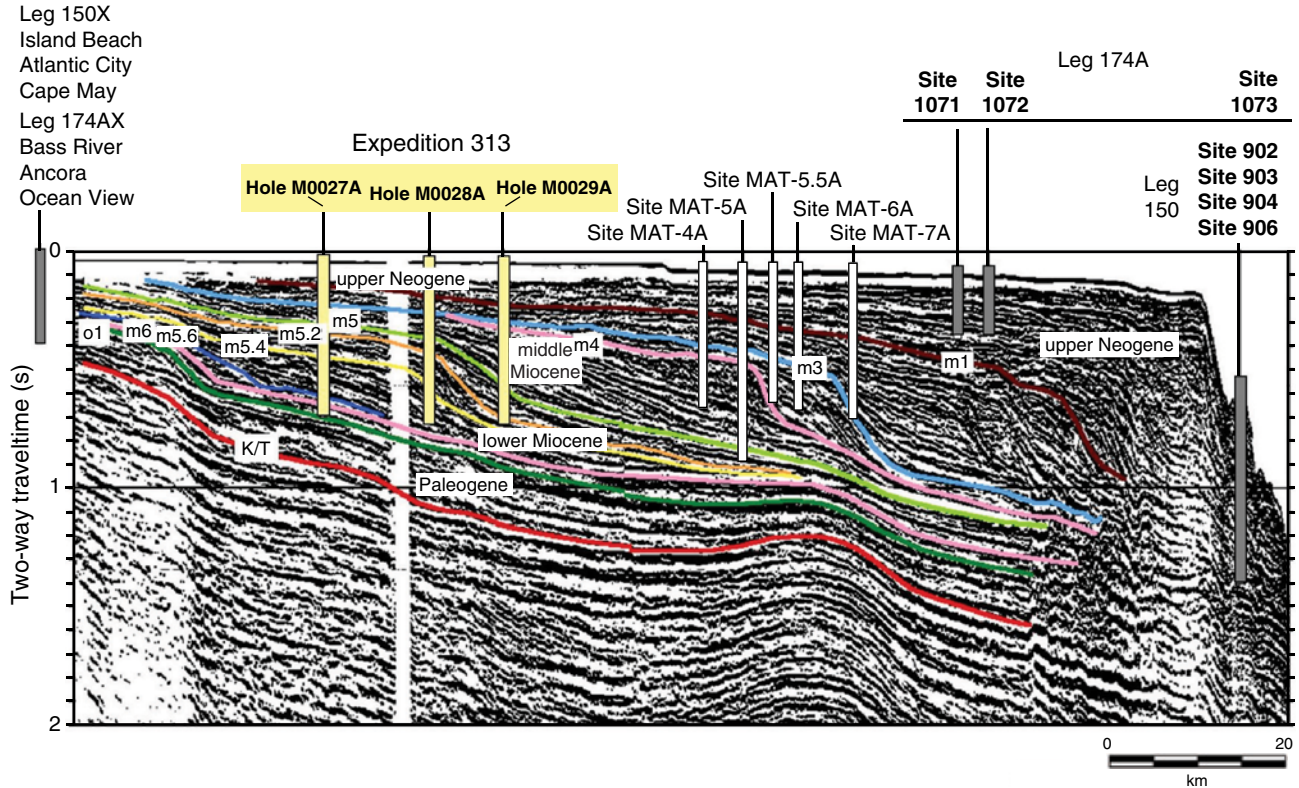
Figure F3. Comparison of Oligocene–Miocene slope sequences, onshore sequences (~0.5 m.y. uncertainty), oxygen isotopes, Bahamian reflections (Eberli et al., 1997), and the inferred eustatic record of Haq et al. (1987). (After Miller et al., 1998.) Approximate age error = ~0.5 m.y. of the above sequences.
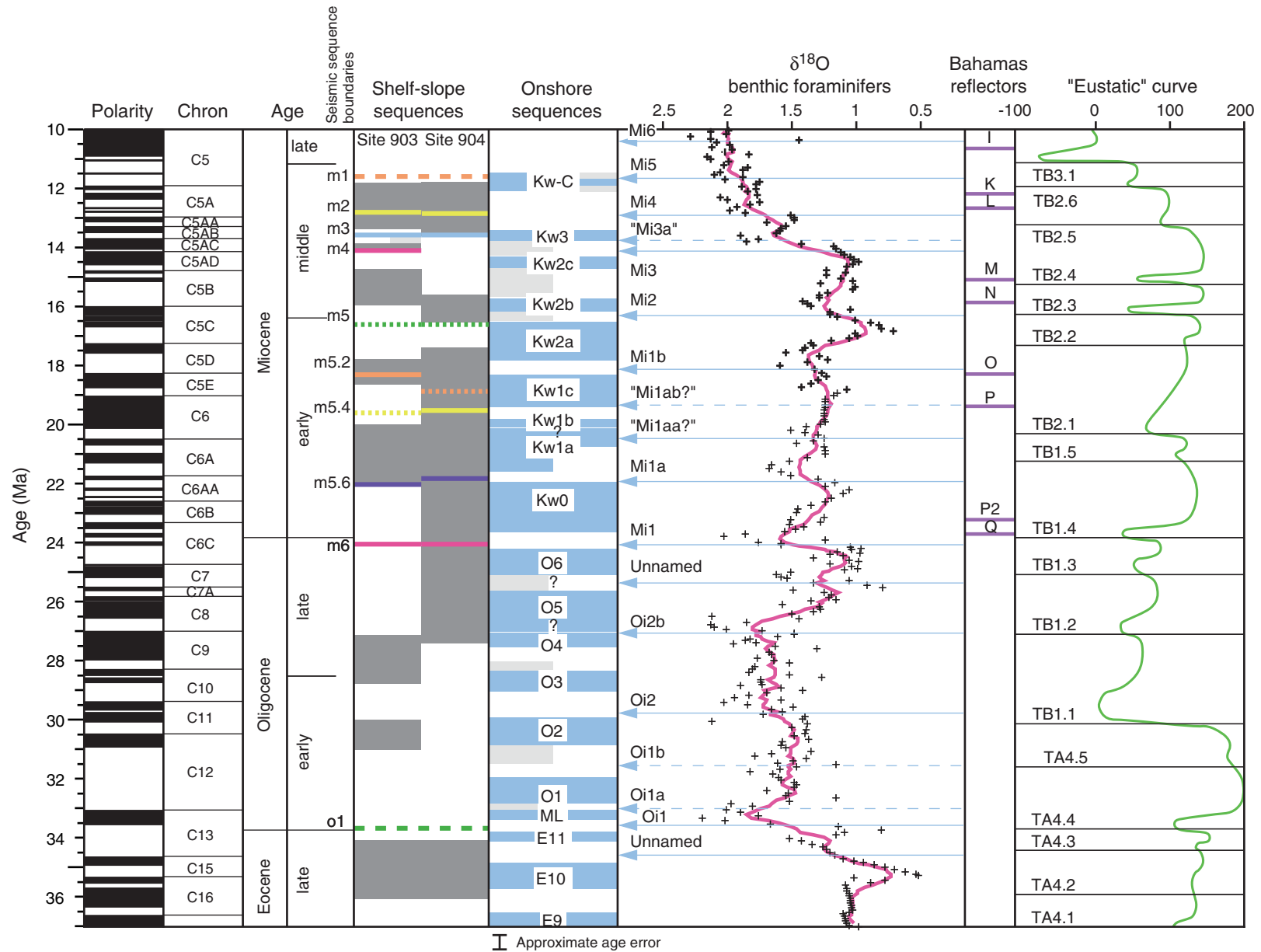
Figure F4. Global sea level (light blue) for the interval 7–100 Ma derived by backstripping data from onshore boreholes along the New Jersey coastal plain. Global sea level (purple) for the interval 0–7 Ma is derived from $\delta^{18}O$. A benthic foraminifer $\delta^{18}O$ synthesis from 0 to 100 Ma (red curve; scale on bottom axis in permil reported to *Cibicidoides* values [0.64‰ lower than equilibrium]) is shown for comparison. Pink box at ~11 Ma = sea level estimate derived from the Marion Plateau (see text). Heavy black line = long-term fit to the backstripped curve. Pale green boxes = times of spreading rate increases on various ocean ridges. Dark green box = opening of Norwegian-Greenland Sea and concomitant extrusion of Brito-Arctic basalts. NHIS = Northern Hemisphere ice sheets. (After Miller et al., 2005a.)
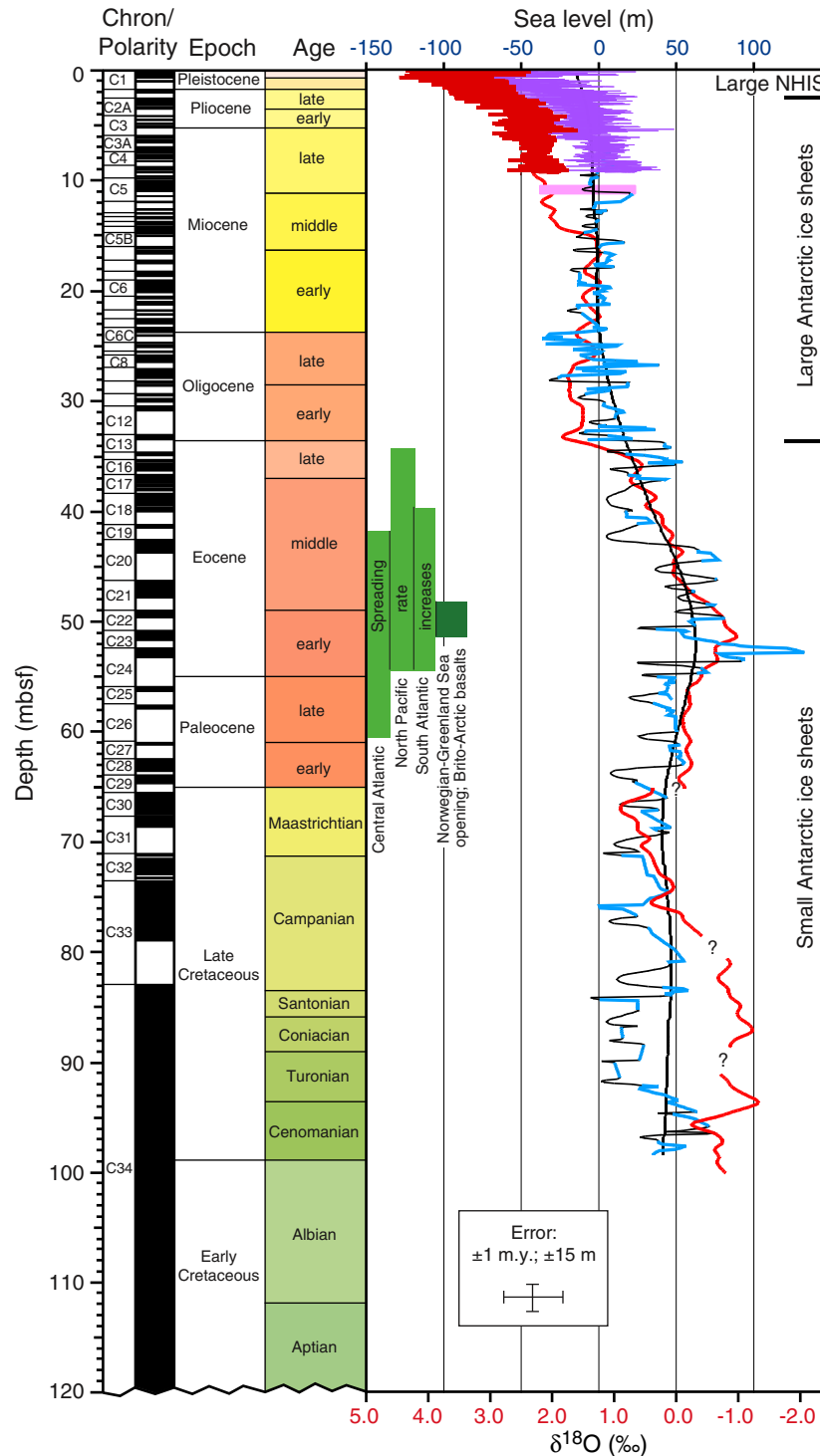
Figure F5. Oc270 dip line 529. CDP = common depth point.
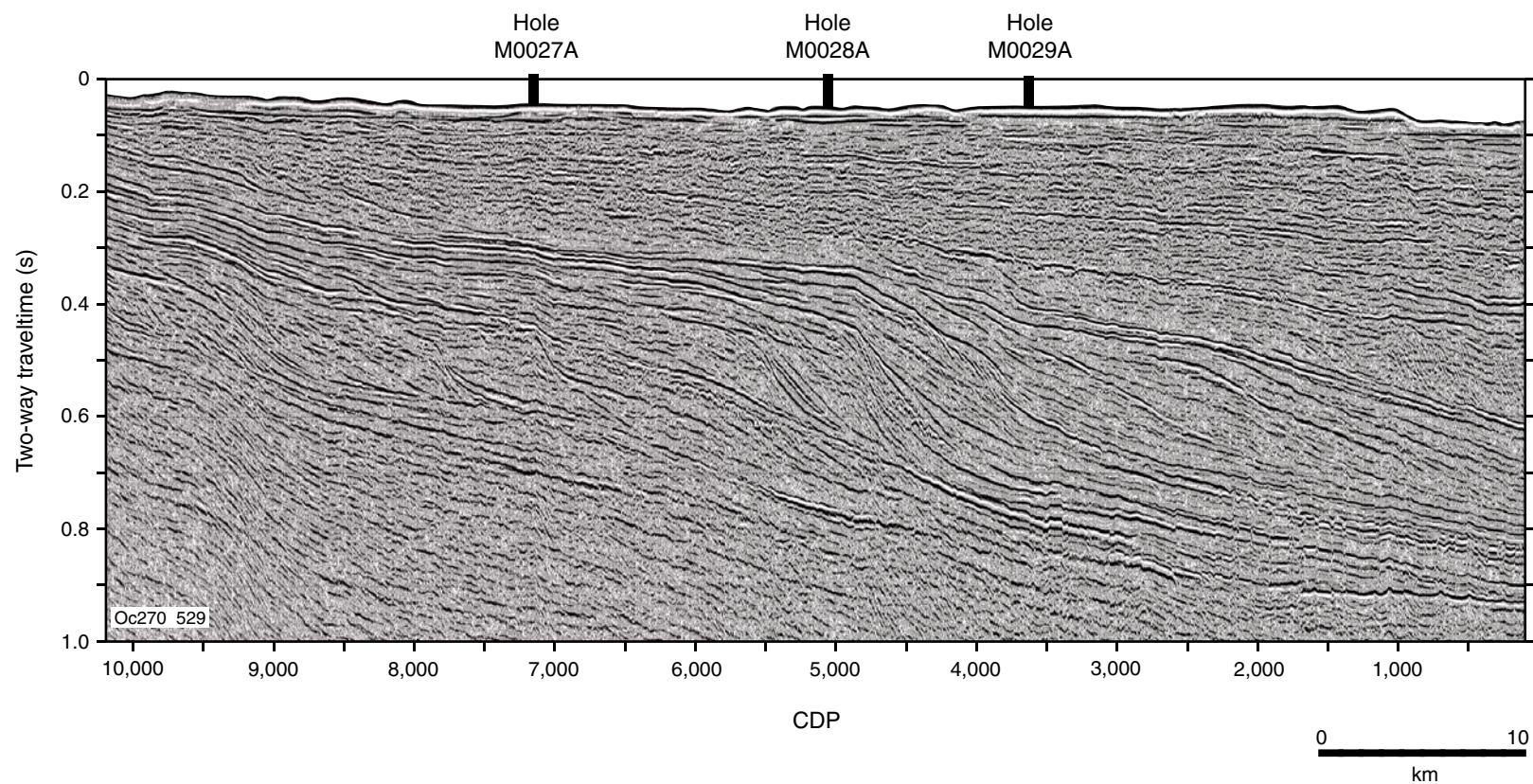
Figure F6. Idealized locations of a three-hole transect to determine the time and magnitude of the base-level fall associated with sequence boundary SB2. This transect samples the youngest sediments below SB2 (Hole M0027A), the oldest sediments above SB2 (Hole M0028A), and more distal sediments above SB2 to ensure dateable material and provide additional backstripping information (Hole M0029A). Bio- and lithofacies will evaluate predicted models of clinoform evolution. Because of the stacked arrangement of sequences offshore New Jersey, several clinoforms can be sampled at one location. HST = highstand systems tract, TST = transgressive systems tract, LST = lowstand systems tract.
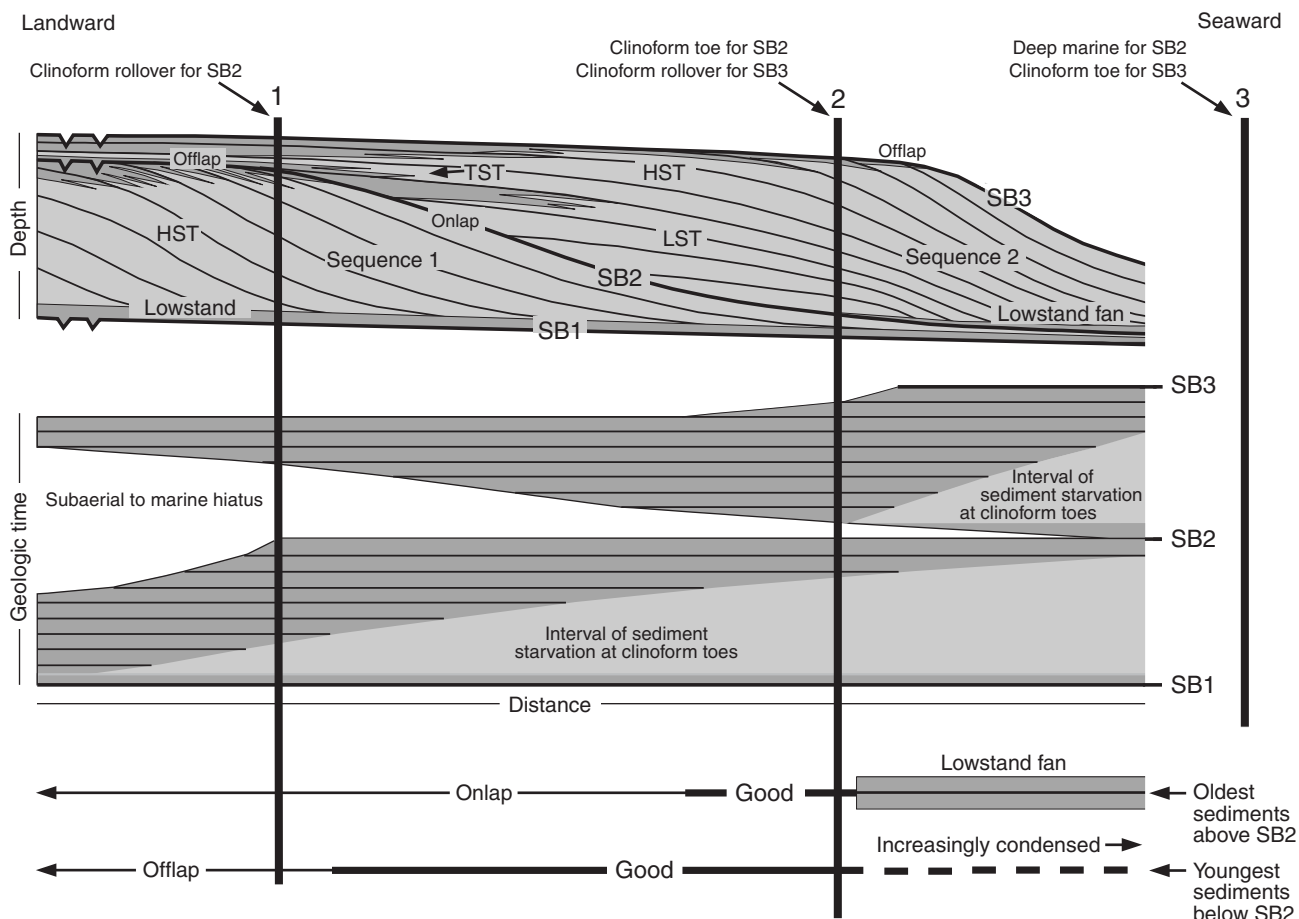
Figure F7. Bathymetry and tracks of MCS profiles in the vicinity of Holes M0027A–M0029A. Holes M0027A–M0029A lie on Oc270 dip line 529 (Fig. **F5**), as well as on the center line of each detailed seismic grid from cruise CH0698. Proposed alternate sites are at crossings of CH0698 profiles in each grid.
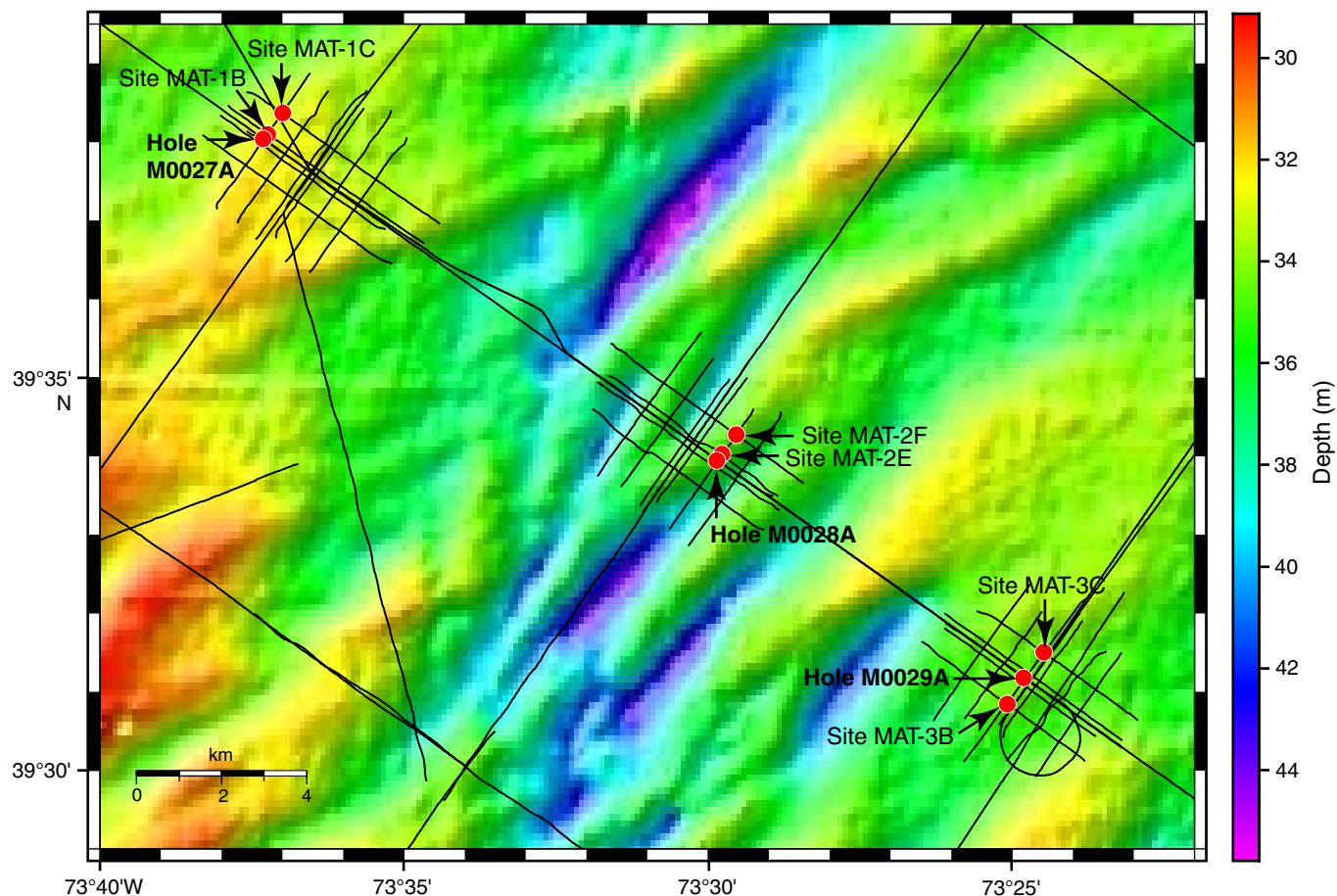
Figure F8. Summary of core recovery, lithologic units, major lithologies, and chloride concentration, Hole M0027A. Grain size for major lithologies increases from left to right. See Figure F4 in the "Methods" chapter for lithology legend.
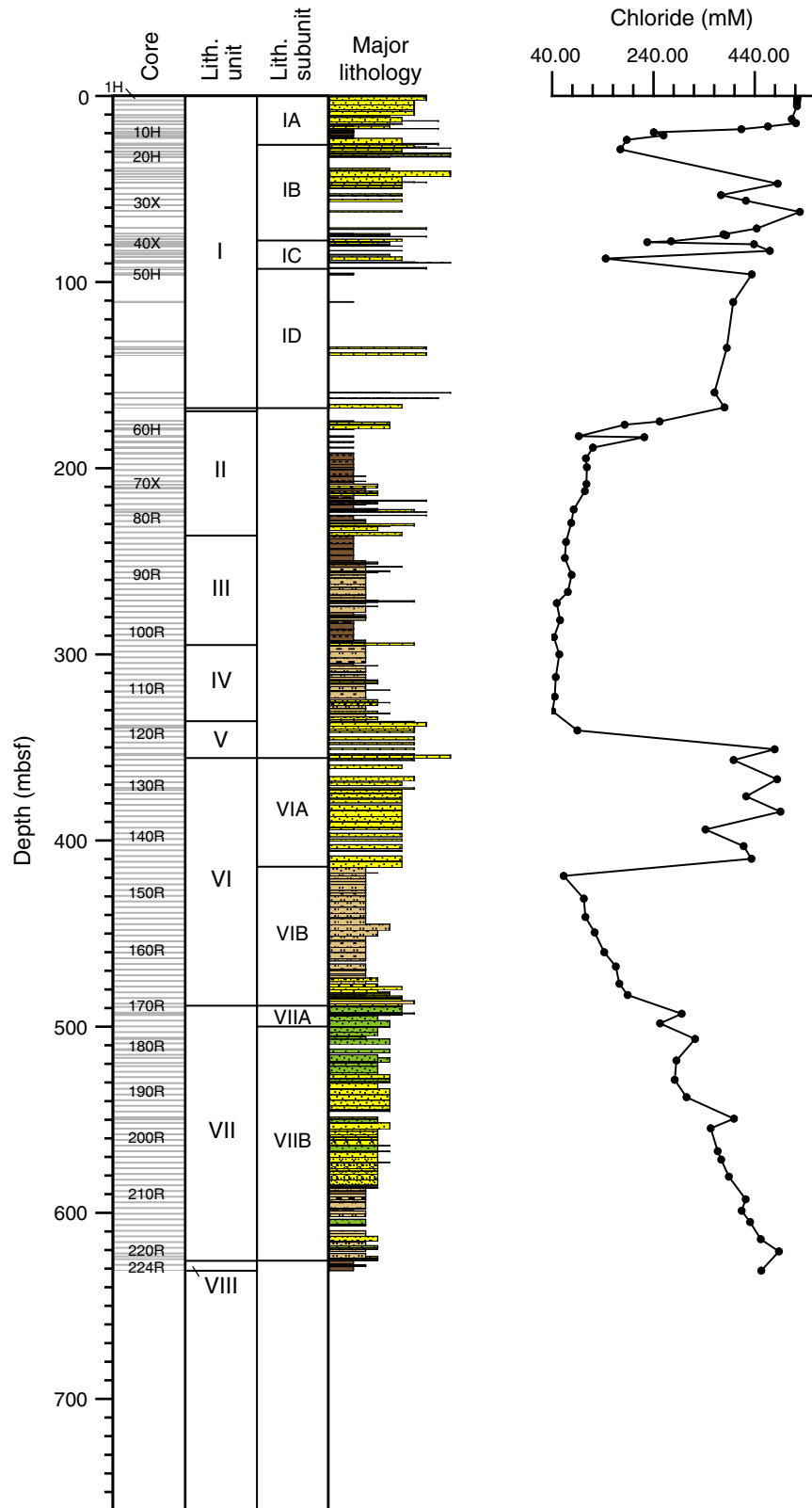
Figure F9. Summary of core recovery, lithologic units, major lithologies, and chloride concentration, Hole M0028A. Grain size for major lithologies increases from left to right. See Figure **F4** in the "Methods" chapter for lithology legend.
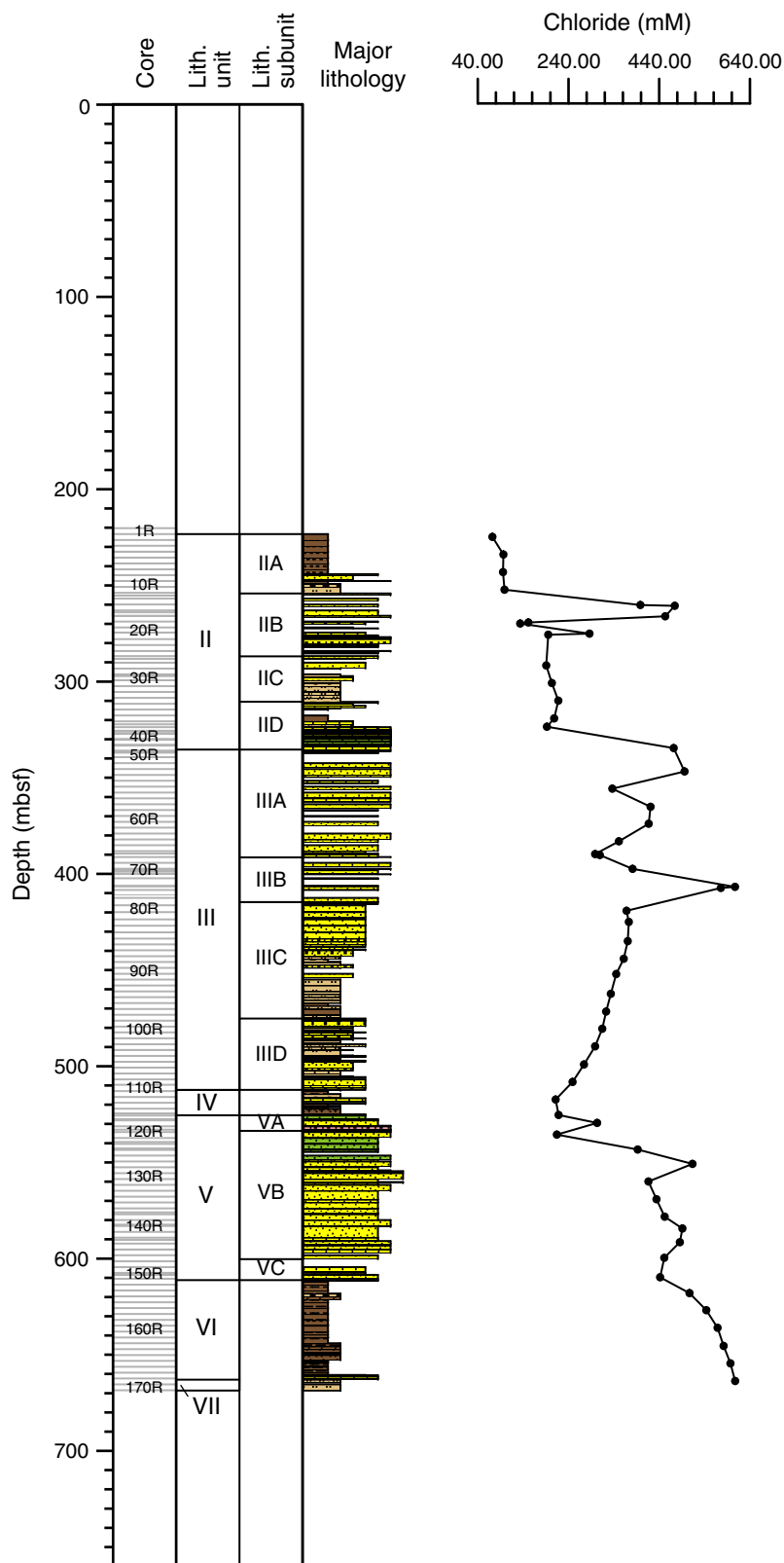
Figure F10. Summary of core recovery, lithologic units, major lithologies, and chloride concentration, Hole M0029A. Grain size for major lithologies increases from left to right. See Figure **F4** in the "Methods" chapter for lithology legend.
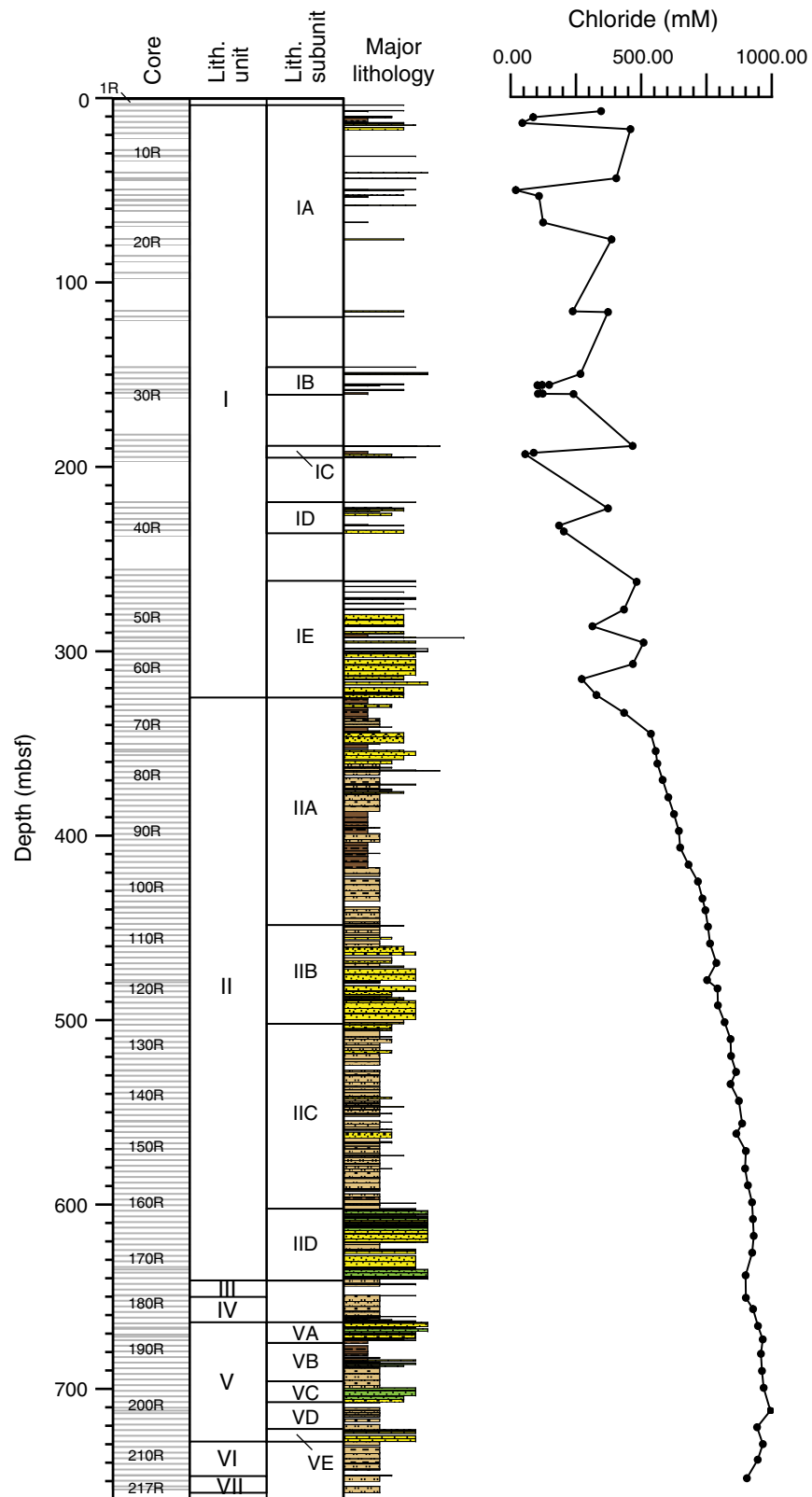
Figure F11. Age assignments based on calcareous nannofossils, planktonic foraminifers, and dinocysts, Hole M0027A.
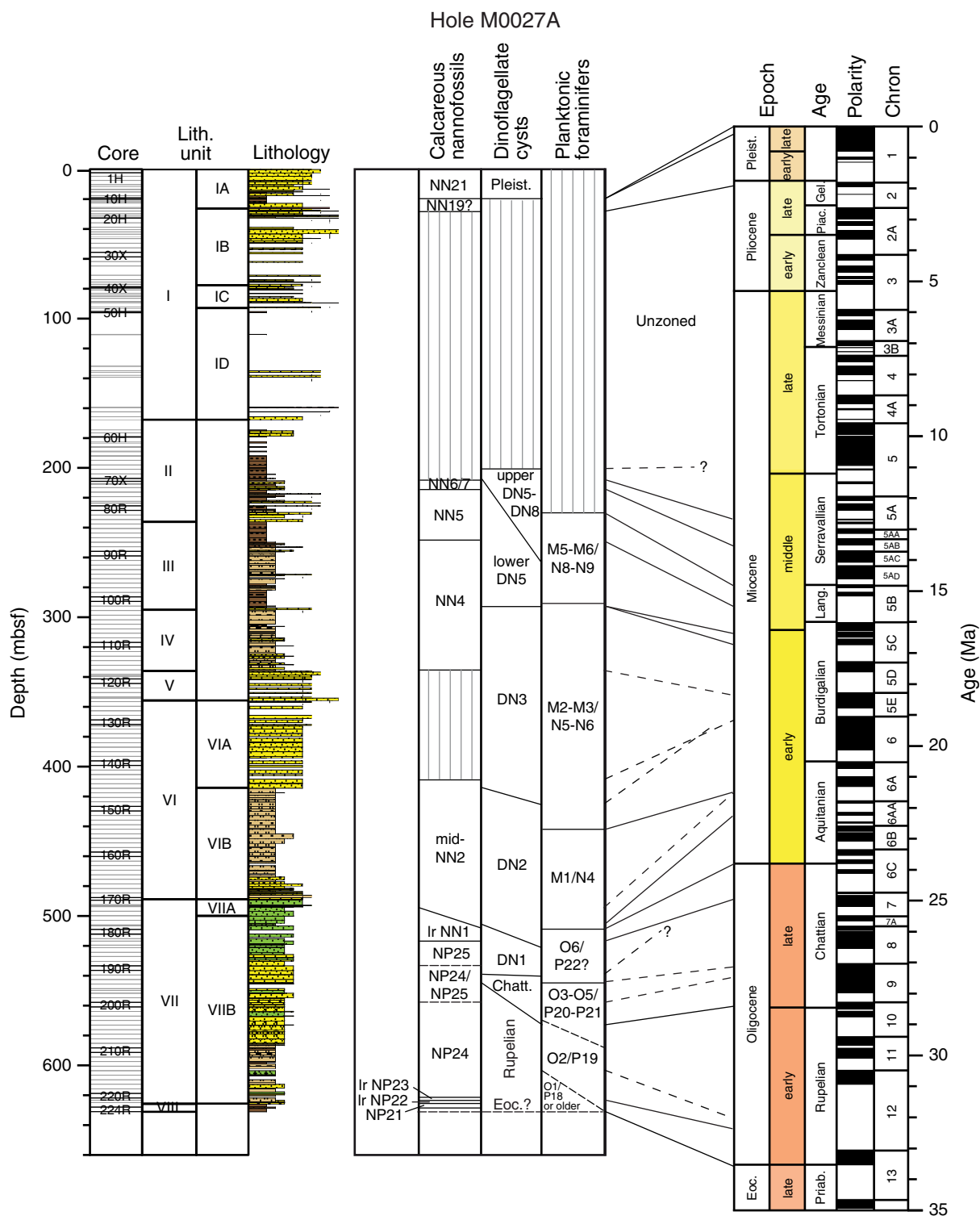
Figure F12. Age assignments based on calcareous nannofossils, planktonic foraminifers, and dinocysts, Hole M0028A.
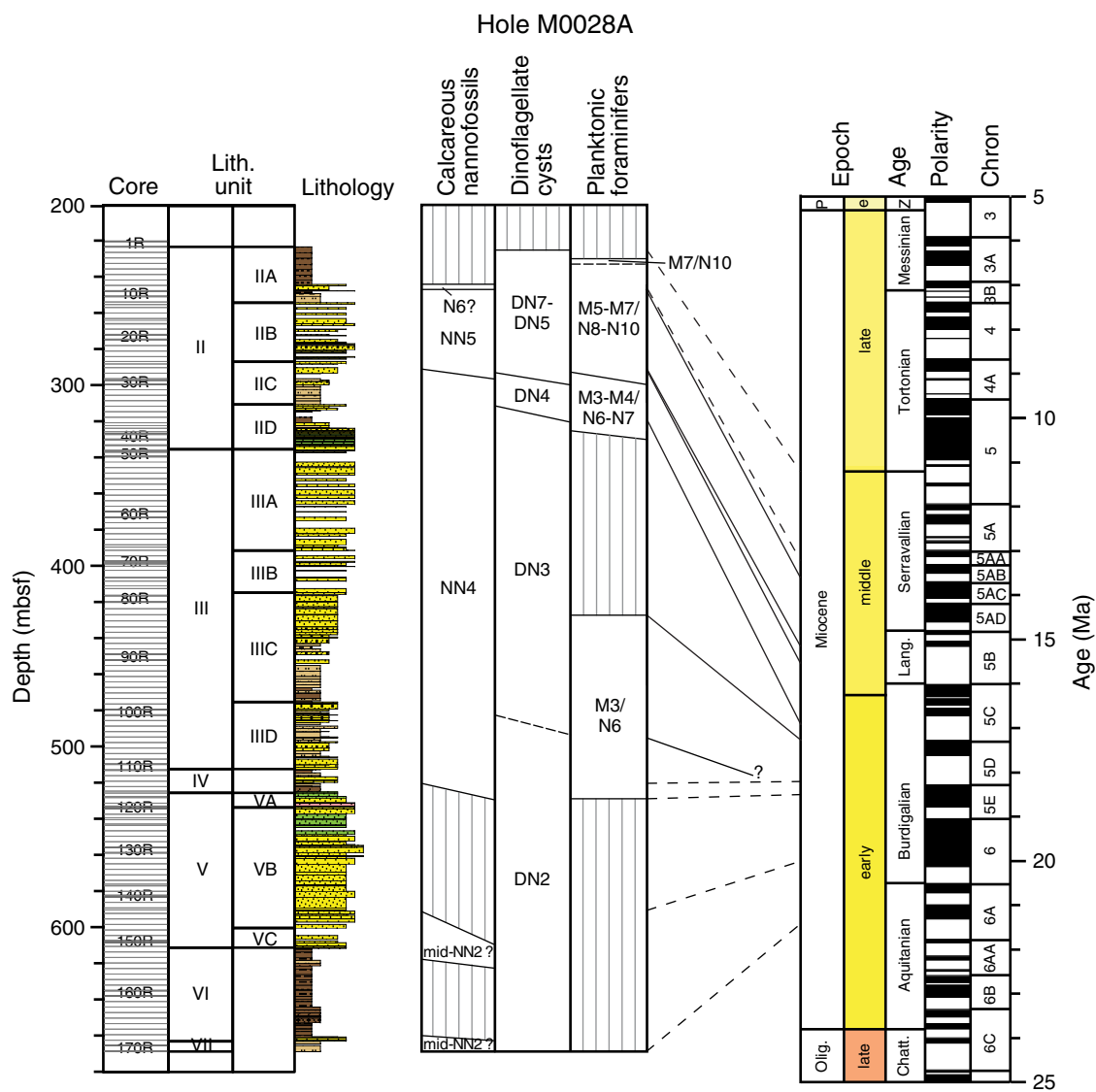
Figure F13. Age assignments based on calcareous nannofossils, planktonic foraminifers, and dinocysts, Hole M0029A.
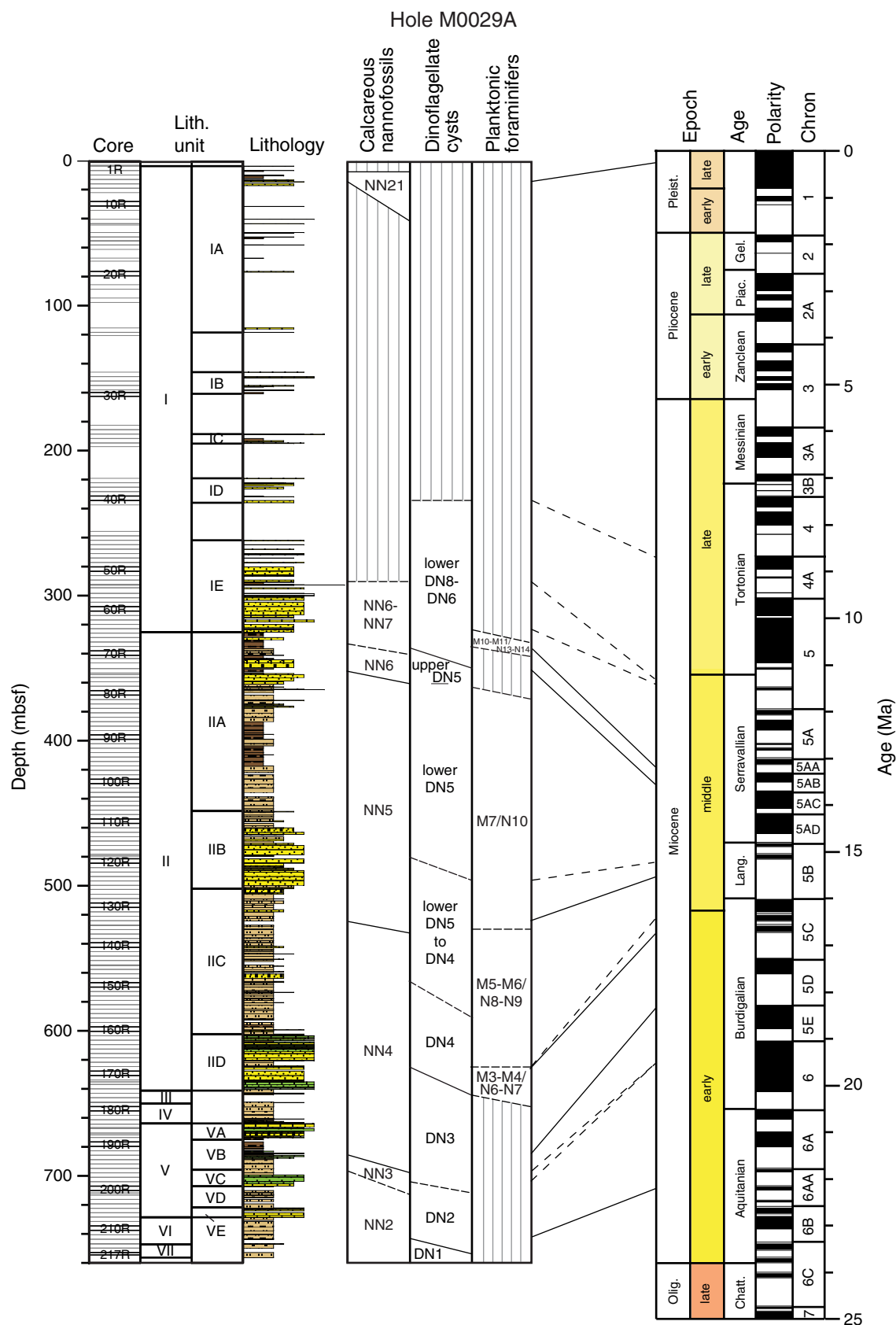
Figure F14. Expedition 313 chronology for the uppermost Eocene? to Pleistocene section based on integrating biostratigraphy and Sr isotopic ages obtained in Holes M0027A–M0029A. Planktonic foraminifer M zones from Berggren et al. (1995), planktonic foraminifer E and O zones from Berggren and Pearson (2005), nannofossil zones from Martini (1971), and dinocyst zones from de Verteuil and Norris (1996). Geomagnetic polarity time-scale from Cande and Kent (1995).
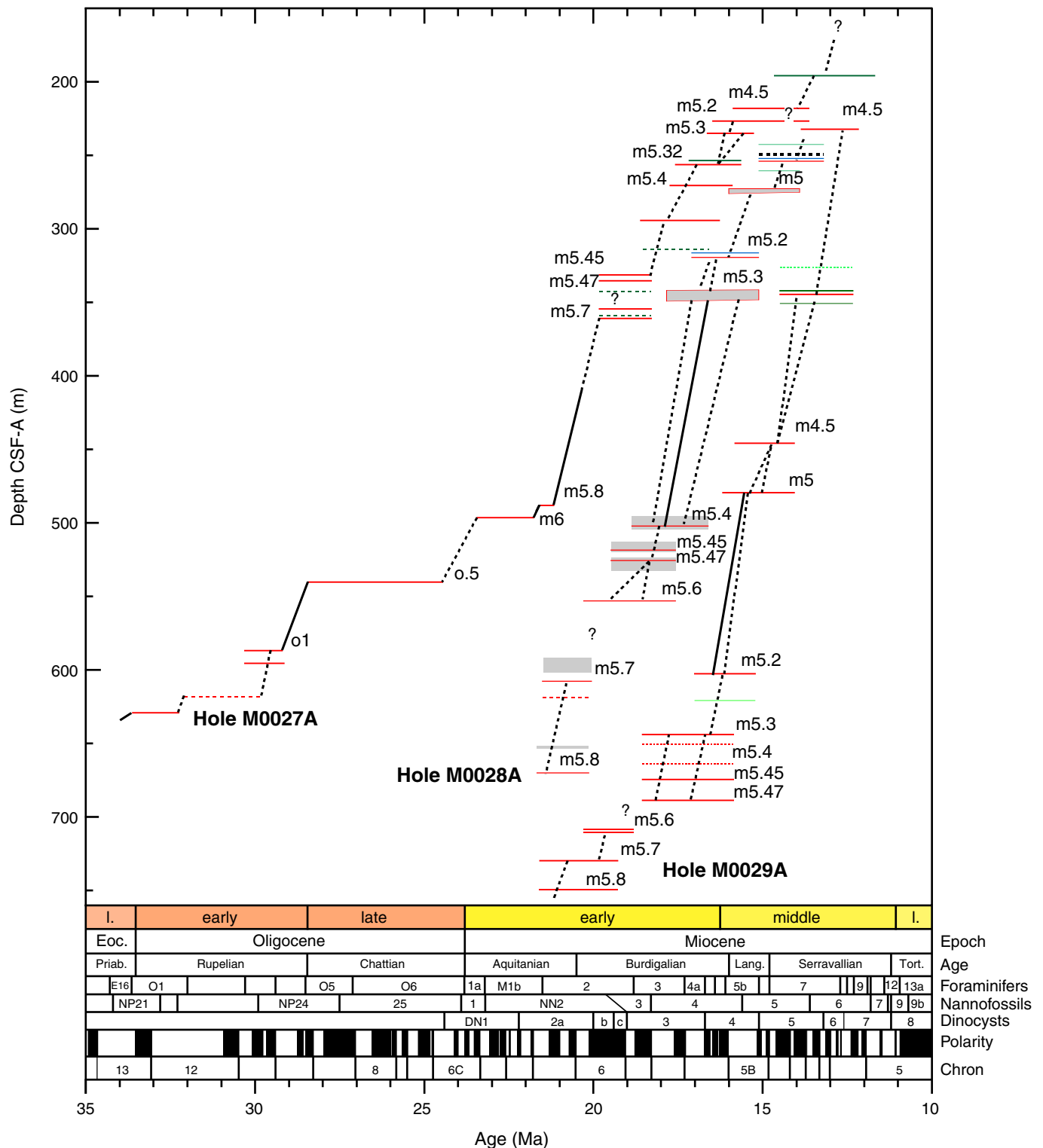
Figure F15. Graphic summary of downhole measurements collected offshore during Expedition 313. Open-hole logging was planned and carried out in stages beginning with the lower section of each borehole. Sediments in the upper ~200 m of each hole were generally unstable. Deterioration of these shallow portions during the early stages of logging the deepest intervals may have contributed to difficulty pulling pipe. Gray reflectors were traced from Oc270 MCS line 529 (see Fig. **F16**); two-way traveltimes have been converted to depths below seafloor and are shown to the left of each drill site. Vertical seismic profile (VSP) and through-pipe gamma logs are displayed to the left of the actual position of each borehole. Open-hole logs are shown to the right. Colored vertical bars show approximate positions of logs.
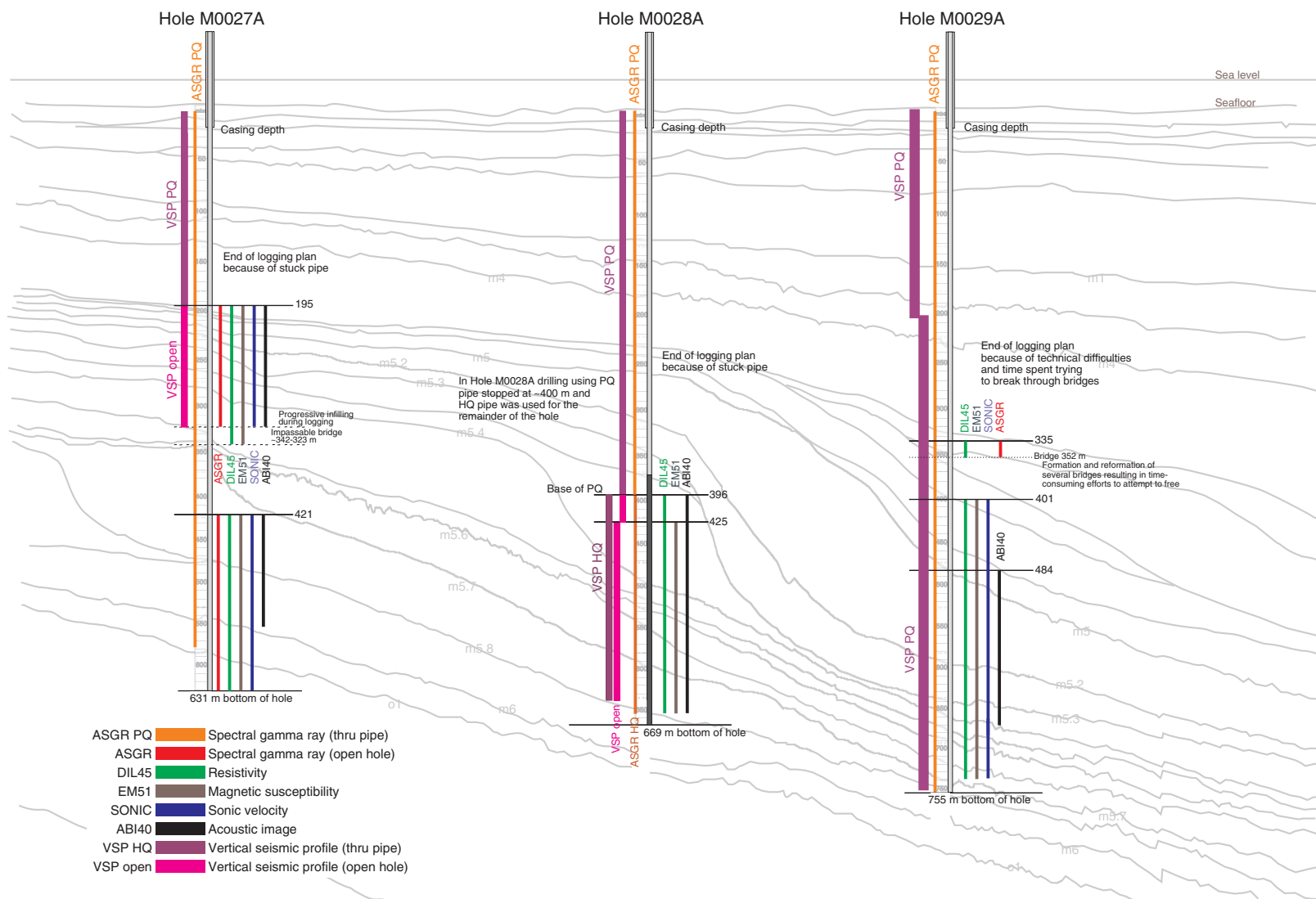
Figure F16. Reflectors on Oc270 line 529 through Holes M0027A–M0029A showing drilled depths at each site. Seismic sequence boundaries traced across the available seismic grid are labeled. CDP = common depth point.
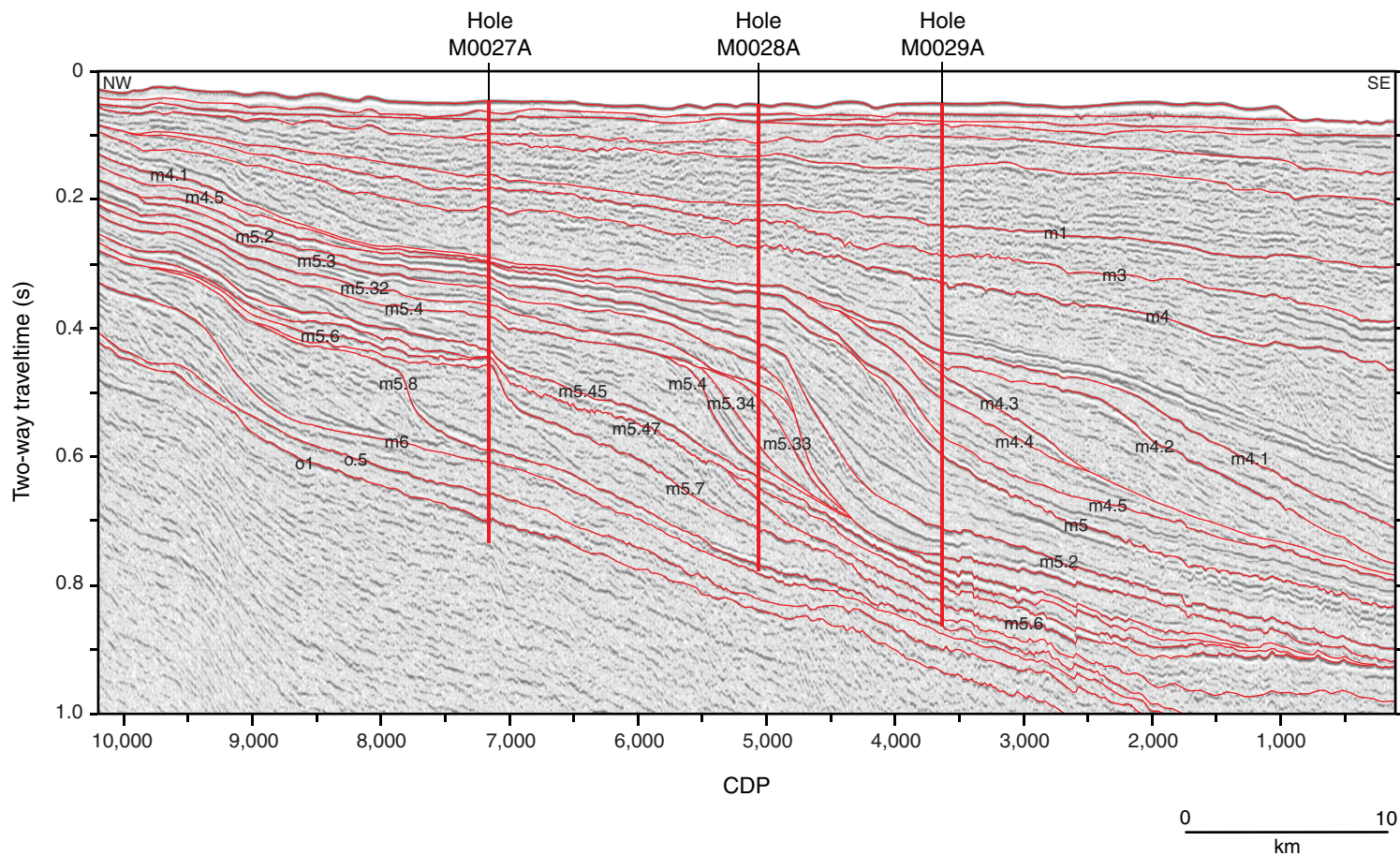
Table T1. Expedition 313 operations summary.

Hole	Latitude	Longitude	Water depth (mbsl)	Number of cores (runs)	Interval cored (m)	Core recovered (m)	Core recovery (%)	Penetration (mbsf)	Hole recovery (%)	Time on site (days)
M0027A	39°38.046067'N	73°37.301460'W	33.53	224	547.01	471.59	86.21	631.01	74.74	22.0
M0028A	39°33.942790'N	73°29.834810'W	35.05	171	476.97	385.50	80.82	668.66	57.65	28.7
M0029A	39°31.170500'N	73°24.792500'W	35.97	217	609.44	454.31	74.55	754.55	60.04	26.3
			Totals:	612	1633.42	1311.40	80.29		63.77	77.0

Table T2. Location of description and measurements made during Expedition 313. (**See table notes.**)

L/B Kayd, offshore New Jersey	Onshore Science Party, Bremen

Core description:
  Core catcher description
	Core description:
	  Split-core visual core description

Core photography:
  Core catcher photography
	Core photography:
	  Full core and close-up photography

Whole-core multi-sensor logging:
  Density
  Velocity
  Magnetic susceptibility
  Electrical resistivity
	Discrete sample index physical properties:
	  Compressional *P*-wave velocity
	  Bulk, dry, and grain density
	  Water content
	  Porosity and void ratio

Geochemistry:
  pH by ion-specific electrode
  Alkalinity by single-point titration to pH
  Ammonium by conductivity
  Chlorinity by automated electrochemical titration*
	Geochemistry:
	  IW analysis by ICP-AES and IC
	  Sediment TOC, TC, and TS by LECO (carbon-sulfur analyzer)
	  Sediment mineralogy by XRD

Downhole logging:
  Spectral natural gamma ray
  Induction resistivity
  Full waveform sonic
  Optical imaging
  Acoustic imaging
  Acoustic caliper
  Electrical conductivity
  Vertical seismic profiling
	Micropaleontology:
	  Calcareous nannofossils
	  Benthic foraminifers
	  Planktonic foraminifers
	  Marine palynology (dinocysts)
	  Terrestrial palynology (pollen and spores)
	
	Other:
	  Natural gamma ray (on cores)
	  Thermal conductivity
	  Color reflectance of split-core surface at discrete points
	  Continuous digital line scanning of split-core surface
	  CT scanning (selected cores only)
	  Discrete paleomagnetic measurements

Notes: * = conducted prior to the Onshore Science Party at the University of Hawaii. ICP-AES = inductively coupled plasma–atomic emission spectroscopy, IC = ion chromatography, TOC = total organic carbon, TC = total carbon, TS = total sulfur, XRD = X-ray diffraction, CT = computed tomography.